


Spring 2021

Quantum optics, entanglement, and Bell's Theorem

Andrew D. Poverman
Bard College

Follow this and additional works at: https://digitalcommons.bard.edu/senproj_s2021

 Part of the [Atomic, Molecular and Optical Physics Commons](#), and the [Quantum Physics Commons](#)



This work is licensed under a [Creative Commons Attribution-Noncommercial-No Derivative Works 4.0 License](#).

Recommended Citation

Poverman, Andrew D., "Quantum optics, entanglement, and Bell's Theorem" (2021). *Senior Projects Spring 2021*. 211.

https://digitalcommons.bard.edu/senproj_s2021/211

This Open Access is brought to you for free and open access by the Bard Undergraduate Senior Projects at Bard Digital Commons. It has been accepted for inclusion in Senior Projects Spring 2021 by an authorized administrator of Bard Digital Commons. For more information, please contact digitalcommons@bard.edu.

Quantum optics, entanglement, and Bell's Theorem

A Senior Project submitted to
The Division of Science, Mathematics, and Computing
of
Bard College

by
Andrew Poverman

Annandale-on-Hudson, New York
May, 2021

Abstract

The field of quantum optics provides a wonderful setting in which to study fundamental aspects of quantum mechanics such as entanglement, Bell's theorem, and non-locality. This thesis presents theoretical discussions of qubits, entanglement, and Bell's theorem in addition to experimental discussions on the nature of photons, creating entangled states using Spontaneous Parametric Down-Conversion (SPDC), and a Bell Test with polarization entangled photons. The experimental sections are written to be useful as instructions for one to conduct these experiments on their own. By doing these experiments, one will gain familiarity with quantum optics experiments as well as a firmer grasp on the intricate nature of measurements in quantum mechanics. On the topic of measurement, there is a brief discussion on the von Neumann model of measurement and the concept of decoherence.

Contents

Abstract	iii
Dedication	vii
Acknowledgments	ix
1 Introduction	1
2 Qubits	5
2.1 Single Photon Mach-Zehnder Interferometer	5
2.1.1 Phase Shifts	6
2.1.2 Matrix Representation	8
2.2 Two-level Atoms	15
3 Entanglement	21
3.1 Formalism	21
3.2 Examples	26
3.2.1 Basis Dependence	26
3.2.2 Polarization Entanglement	28
4 Generating Down-Converted Photon Pairs	37
4.1 Spontaneous Parametric Down Conversion	37
4.2 Optical Alignment Procedure	42
4.2.1 Generating and Detecting Down Converted Photons	45
5 Hanbury Brown-Twiss Experiment	49
5.0.1 Theory	50
5.0.2 Experimental Procedure	52
5.0.3 Results and Discussion	54
6 Bell's Theorem and Testing the Bell Inequality	57

6.1	Introduction to Bell's Theorem	57
6.1.1	The Bell Inequality	58
6.1.2	Thought Experiment Version of Bell's Inequality	65
6.2	Bell Test Experimental Procedure	69
6.2.1	Results and Discussion	72
6.3	Von Neumann Model of Measurement and Decoherence	73
6.3.1	Brief Discussion of Decoherence	77
7	Conclusion	81
8	Appendix	85
8.1	Appendix A. Digitizer Settings	85
8.2	Appendix B. Quartz Crystal Thickness	90
8.3	Appendix C. Relevant Parts List	92
	Bibliography	93

Dedication

To my sister Rachel.

Acknowledgments

I am grateful to my advisors Matthew Deady, Hal Haggard, and Antonios Kontos who have each greatly influenced the way I perceive physics, mathematics, and philosophy. I would like to thank Matt for his endless support and for always reminding of my capabilities. I thank Hal for our many discussions and for showing me how to collect my knowledge and approach my questions systematically. As well, I thank Antonios for creating an awesome lab environment in which to learn the ways of an experimentalist and for all of the time spent in the GOlab building experiments and collecting data. Without Antonios' curiosity and guidance, these experiments would not have happened. I would also like to thank all my friends, and especially Nathalie and Yan for their genuine kindness and support over the years. Much love to all.

“Scientists are seeking something that is much more significant to them than pleasure. One aspect of what this something might be can be indicated by noting that the search is ultimately aimed at the discovery of something *new* that had previously been *unknown*. But, of course, it is not merely the novel experience of working on something different and out of the ordinary that the scientist wants — this would indeed be little more than another kind of “kick”. Rather, what [they are] really seeking is to learn something new that has a certain fundamental kind of significance: a hitherto unknown lawfulness in the order of nature, which exhibits *unity* in a *broad range* of phenomena. Thus, [they wish] to find in the reality in which [they live] a certain oneness and totality, or wholeness, constituting a kind of *harmony* that is felt to be beautiful. In this respect, the scientist is perhaps not basically different from the artist, the architect, the musical composer, etc., who all want to *create* this sort of thing in their work.”

— David Bohm

1

Introduction

In many ways, undergraduate quantum mechanics courses expose the student to a catalog of simplified examples that provide a strong connection between the necessary mathematical tools and physical concepts needed to solve textbook problems, but without giving the student much in the way of philosophical or conceptual tools through which they can devise their own questions on the topic. This is not by fault of the many great professors of physics, but rather that the philosophical foundations of quantum mechanics is a vast realm of study on its own, and to introduce it properly would require at least a semester long course. Thus the aim of this text is to present just one unique aspect of quantum mechanics, the phenomenon of entanglement, in a manner that attempts to construct a bridge between a commonly studied quantum system and the philosophical foundations of quantum mechanics such as Bell's theorem and the concept of measurement. This text also strives to present some of the more abstract mathematics of quantum mechanics such as Hilbert spaces and interesting features of entangled states that are often glossed over in many introductory texts. By doing so, several common misconceptions regarding entangled states and composite systems will be dispelled. Furthermore, this text presents three different experimental sections that connect physical results to the theoretical frameworks commonly presented in a quantum mechanics course. These experiments are presented in the context of quantum optics, a very accessible regime to conduct fundamental tests of quantum mechan-

ics, and are intended to be useful as lab guides for undergraduate students in an advanced lab course who wish to deepen their understanding of the subject by way of conducting experiments. Using the experimental apparatus presented in this text, one will be able to conduct a variety of experiments such as a Hanbury Brown-Twiss test and a Bell test. By making these connections between theory, experiment and briefly quantum foundations, I hope to provide a guide through which a more advanced undergraduate physics student may refine their understanding of these subtle aspects of quantum theory, especially in regards to entanglement, non-locality, and the concept of quantum measurement. I hope that by drawing connections between experimental results and theoretical predictions in a manner that differs from many introductions to quantum mechanics, the reader will be given a new lens through which to conceptualize the more dense and often confusing discussions of this subject.

Chapter 2 presents the mathematical formalism of qubit systems by way of two examples. The first example will be an in depth discussion regarding a single photon in a Mach-Zehnder Interferometer. This example highlights the probabilistic nature of quantum mechanical measurements as well as introducing the reader to viewing the photon as a particle rather than a classical wave. After this, there is a brief presentation of the two-level atom. The main function of this example is to reveal the almost ubiquitous nature of the qubit formalism as well as give a slight introduction to quantum operators (the time evolution operator and Pauli operators). This chapter will prepare the reader to utilize the qubit formalism in order to engage with the theory behind quantum entanglement.

Chapter 3 discusses the mathematical framework behind entanglement. In doing so, the reader will be introduced to the idea of Hilbert spaces as well as composite systems. Then, there is an introduction to entangled states that will lead to a proof that entangled state vectors cannot be written as the product of single particle state vectors. Then the reader is given some examples that are aimed to illuminate some subtle qualities of entanglement and hopefully dispel one or two very common misconceptions regarding entanglement. To finalize this chapter, there is a

mathematical discussion of polarization entangled photons as this is the physical system that is central to doing a Bell Test presented later in the text.

Chapter 4 initiates the experimental discussion that accompanies the theoretical topics covered in the previous chapters by presenting an experimental procedure for generating correlated down-converted photon pairs via Type-I Spontaneous Parametric Down-Conversion (SPDC). As well, there is a discussion on how to optimize the detection of down-converted pairs. Additionally, a bit of theory behind SPDC will be presented, specifically in regards to the beta barium borate (BBO) non-linear crystal being used to produce photon pairs.

Chapter 5 builds on the experimental set-up presented in chapter 3 to conduct a Hanbury Brown-Twiss test. This chapter presents the theory and conceptual relevance of measuring the second order correlation function as a way of confirming the particle nature of single photons being produced by the apparatus. Then there is a presentation and discussion of the experimental results that reveals the statistical nature of performing quantum optics experiments.

Chapter 6 further develops the experimental set-up in order to test Bell's inequality. There is a derivation of the Bell inequality in the form that John Bell first derived as well as the more experimentally accessible form derived by Clauser, Horne, Shimony, and Holt. There is also a brief discussion regarding the assumptions of the EPR thought experiment and how these can lead to Bell inequalities. This is followed by the experimental procedure for conducting a Bell Test using the experimental set-up developed throughout this thesis as well as a discussion of experimental results.

In addition to extending the common method of presenting quantum mechanics to undergraduates, this research has been greatly motivated by the work of physicists and philosophers of science who have challenged and dissected quantum theory from its inception. One of the most prominent examples of this is the famous Einstein-Podolsky-Rosen (EPR) paradox presented as a thought experiment (or gedankenexperiment in German) in a paper published in 1935. In principle, the EPR argument begins with a few guiding philosophical assumptions regarding the nature of physical reality, and from these, EPR argue that quantum mechanics must be

an incomplete theory. This led to a decades long struggle to try and reconcile this possibility and begin studying the foundations of quantum mechanics in such a way as to reconstruct a more complete theory of reality. This led physicist John Stewart Bell, from Northern Ireland, to begin looking into the works of notable physicists David Bohm and John von Neumann in search of a better understanding of the mysteries of interpreting quantum mechanics as a physical theory. This inspired Bell to write his famous paper, pre-printed in 1964 and published in 1966 after being misfiled, that presented the now well-known Bell inequality¹. This presentation of Bell's theorem and the Bell inequality sparked a reaction (although somewhat delayed) by the physics community to try and develop experimental tests to confirm once and for all the completeness of quantum theory. In the end, the most accessible experiments of this nature involved optics experiments using single photon sources to produce polarization entangled states, and now in the present moment these kinds of experiments are still the most accessible way of experimentally learning about quantum mechanics and the subtleties of entanglement and statistical measurements in a non-local framework. In the end, these experiments are aimed to provide the student with a hands on experience that will grant them a form of understanding that comes from actually *seeing* rich physics occur by way of setting up delicate experimental apparatuses and analyzing statistical data. Thus any student who conducts these experiments will have no more doubt regarding the nature of reality in the quantum context.

¹For more details on this crazy story of how one of the most influential papers in modern physics was misfiled by the journals editor, see Jammer, *The Philosophy of Quantum Mechanics* (John Wiley & Sons, Inc, 1974), 303.

2

Qubits

The aim of this chapter is to introduce a mathematical framework that can be used to study any two-state quantum system. Each system encountered in this chapter is an example of a *qubit*, which is a term coined by physicist Benjamin Schumacher to describe one of the “simplest” quantum systems. Having a strong conceptual and mathematical understanding of qubits will be useful in later chapters as this formalism is directly applied to the study of entangled systems. This section provides two examples of qubit systems that will put the mathematical formalism into a physical context. First is an examination of a photon in a Mach-Zehnder Interferometer and second is an example of two-level atoms.¹

2.1 Single Photon Mach-Zehnder Interferometer

In general, an interferometer is a kind of optical device that restricts light to a finite number of discrete beam paths. These beams can undergo a series of transformations by interacting with various optical components, but when the beam paths are recombined into a single beam, it is possible to observe interference patterns. With a classical laser beam, this would mean that one can set up detectors at the ends of the various beam paths and detect the intensity

¹For more qubit examples, see Schumacher & Westmoreland Chapter 2.
Schumacher & Westmoreland, *Quantum Processes, Systems, & Information* (Cambridge University Press, 2010), 15.

of the light at each detector to learn something about how the light has been altered by the interferometer. The kind of interferometer we will consider in the following example is the *Mach-Zehnder interferometer* (MZI) seen in Fig. 2.1.1.

With an electromagnetic wave traveling through the two beams of the MZI, we said that there will be macroscopic interference patterns that we can observe by placing a screen or detector at the outputs of the interferometer. To put things solely in the context of quantum mechanics, one may want to ask the question: Instead of using an electromagnetic wave, what happens when we send a single photon through an MZI? Right off the bat, there are some interesting subtleties within that question alone. For one, how does a single photon interact with optical components such as mirrors and beam splitters? Do they act the same as electromagnetic waves incident on the optical devices? And even more perplexing: What does it mean to have interference effects when you only send in one photon at a time? Quantum mechanics will have the answers for us, but they may cast an entirely new perspective on what it means to think of interference effects and interferometer experiments.

2.1.1 Phase Shifts

In general, when light is incident on a surface at which the index of refraction changes, it may travel from one medium to another, and the wave speed in this new medium will change by an amount related to the index of refraction of the material $v_{\text{med}} = \frac{c}{n_{\text{m}}}$ where c is the speed of light in vacuum and n_{m} is the index of refraction of the new material. As well, there may be a change in direction of the wave when propagating in this new medium related to Snell's Law. In every case where a light wave transfers between mediums, there will be some percentage of the incident light that will be reflected, and with this the reflected wave may pick up some phase change due to the interaction.

Consider the following scenario: There are two materials placed back to back with no space for air or any other material to get in between them. Then, light is incident on the surface of the first material, denoted i , with an index of refraction n_i , and travels through i until it is incident on the second material, denoted r , with an index of refraction n_r . When reaching the second

material r , some portion of the wave will be reflected. When considering possible phase changes during this interaction between light and the materials, there are two cases that can occur:

1. When $n_i < n_r$ (meaning $v_i > v_r$), the reflected wave picks up a phase shift of $\Delta\phi = \pi$ relative to the incident light.
2. When $n_i > n_r$ (meaning $v_i < v_r$), the reflected wave picks up no phase shift relative to the incident light ($\Delta\phi = 0$).

These results come from treating light as a ray and doing geometrical analysis, and it would be besides the point to show here, but knowing these results will be essential for analyzing the MZI. To contextualize these results, consider the familiar scenario (for anyone who has taken a Modern Physics or Optics course) of light being reflected from a dielectric mirror. The reflective dielectric material has the property $n_r > n_{\text{air}}$, and so $\Delta\phi = \pi$ when light travels through the air and is incident on the mirror (Case 1).

For uncoated glass, when light encounters an air-glass interface, the majority of the light will be transmitted, but when the glass is coated with thin layers of reflective material (such as a dielectric coating), much more of the light will be reflected (how much exactly depends on the coating). When making these reflective mirrors using glass, the reflective coating could either be applied to the front face of the mirror or the back face. These reflective coatings usually have high indices of refraction, and so we can refer back to the two cases described above to see when the light will pick up a phase shift or not. If the coating is placed on the front of the glass, then we have that $n_{\text{air}} < n_{\text{coating}}$ and so the reflected light has phase shift $\Delta\phi = \pi$. However, if the coating is on the back of the glass, then the possibility of a phase shift depends on the relative indices of refraction of the coating and the glass. Of course, if $n_{\text{glass}} < n_{\text{coating}}$, then case 1 applies again, but if $n_{\text{glass}} > n_{\text{coating}}$, then case 2 applies and so $\Delta\phi = 0$. When we are studying the MZI in particular, it is always the case that $n_{\text{glass}} > n_{\text{coating}}$, and so reflections that occur at a glass-coating interface will have no phase shift.²

²Many thanks to Matthew Deady for his detailed notes on the Mach-Zehnder Interferometer.

2.1.2 Matrix Representation

When we send a single photon into an interferometer, results are measured using *single photon detectors* placed at the ends of the possible beam paths. Named aptly, these detectors can register the presence or absence of a photon at a given time. Since we are interested in knowing the chance that a photon is present at a specific detector or another, our calculations will be probabilistic in nature. In practice, another way of asking this question is to say: If we took one hundred photons and sent them, one at a time, through the MZI how many would arrive at one detector and how many would arrive at the other? In principle, this question is asking about the statistics of repeated independent measurements. On paper, we can find the probability that a single photon will arrive at one detector or another, and this could even help us predict the measurement outcome in a real life experiment. However, if we wanted to confirm the predictions of quantum mechanics using a physical MZI, we could not learn any statistical information just by sending one single photon through. Rather, we would need to do many repeated measurements until the statistics become clear as to the chances of a photon arriving at one place or another. It is in this way that conducting quantum optics experiments of this type are fundamentally statistical. In this section, we will see how given certain initial conditions, we can calculate the probability that our various detectors will “click” or not, indicating the presence of a photon along that beam path. As shown in Fig. 2.1.1, there are two possible beam paths for a photon to travel along.

Each one of these paths is assigned amplitudes (possibly complex) α and β respectively. Suppose we were to introduce a detector in the beam path with amplitude α , then the probability P of detecting a photon on that path is $P = |\alpha|^2$. In this sense, these amplitudes differ from the classical amplitude of an electromagnetic wave, and thus we may want to call them *probability amplitudes* to avoid confusion or misconception. Since we know that the photon must be in one of the two paths, it follows that $|\alpha|^2 + |\beta|^2 = 1$, since a probability can be no greater than 1. Given the two possible situations for a single photon and the probability amplitudes associated with each, we can fully describe the single photon in the MZI using vector algebra.

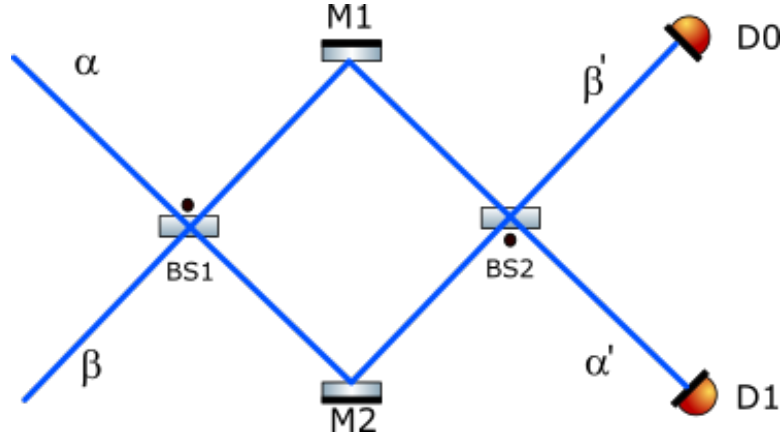


Figure 2.1.1. Mach-Zehnder Interferometer Layout with the upper and lower beams indicated by α and β respectively. The outputs of the interferometer, α' and β' , indicate which beam the photon exits the MZI.

Let us denote the two possible situations for the photon by letters A and B . Further, assign probability amplitude α to situation A and β to situation B . Now, let's say that in situation A , the photon is in the upper beam, and in situation B , the photon is in the lower beam. When the photon is in situation A , the probability amplitude of the upper beam is 1 while for the lower it is 0. This should be self-evident because when the photon is in the upper beam with absolute certainty, there is no chance that it is in the lower beam. Vice versa, in situation B , the probability amplitude of the lower beam is 1 while for the upper it is 0. Given the principle of superposition, we know that while a photon could be in one of these two states with absolute certainty, there is also the possibility of the photon being in some linear combination of the two states. As we will see, this kind of situation may occur, for example, when a photon is incident on a 50/50 beam splitter where the two beam paths of the beam splitter are used for the MZI.

To represent this physical scenario in terms of column vectors, define one situation to be $A = \begin{pmatrix} 1 \\ 0 \end{pmatrix}$ and the other $B = \begin{pmatrix} 0 \\ 1 \end{pmatrix}$. And so, by superposing these two situations by the usual vector addition

$$\alpha \begin{pmatrix} 1 \\ 0 \end{pmatrix} + \beta \begin{pmatrix} 0 \\ 1 \end{pmatrix} = \begin{pmatrix} \alpha \\ \beta \end{pmatrix}, \quad (2.1.1)$$

we can notice that this mathematical representation allows us to write all the possible situations for the single photon as a vector whose elements are probability amplitudes. In this sense, the

two beam paths of the MZI act as a vector basis from which we can write every possible state of a photon in the interferometer. We can see that when $\beta = 0$ we recover situation A , and similarly we recover situation B when $\alpha = 0$. In most non-trivial cases, it is these superpositions of situations which are of particular interest when examining quantum theory.

Not only can we write every possible state of a photon in the interferometer using vectors, but we can also characterize the entire interferometer itself by a 2×2 matrix. In order to find the 2×2 matrix that accurately describes the MZI in particular, we have to look at the matrices describing the individual linear optical elements that make up the interferometer. There are two different optical devices in the most basic MZI: Beamsplitters and mirrors. A balanced beam splitter, or 50/50 beamsplitter (one with equal transmission and reflection coefficients), can be represented by the matrix

$$\mathbf{B}_l = \frac{1}{\sqrt{2}} \begin{pmatrix} 1 & 1 \\ 1 & -1 \end{pmatrix} \quad (2.1.2)$$

where the subscript l is to indicate that a phase shift occurs when the lower beam gets reflected. This was simply a choice as we could have equivalently described a beamsplitter \mathbf{B}_u that adds a phase shift when the upper beam is reflected. In order to make accurate predictions in the lab however, this choice must be consistent with the experimental apparatus. Additionally, full silvered mirrors, which introduce a π phase shift into the beam, can be represented by the matrix

$$\mathbf{M}_{u,l} = \frac{1}{\sqrt{2}} \begin{pmatrix} -1 & 0 \\ 0 & -1 \end{pmatrix} \quad (2.1.3)$$

where now the subscripts indicate the π phase shift on both the upper and lower beams. Notice that both of these matrices are *unitary* meaning that $\mathbf{M}^\dagger \mathbf{M} = \mathbf{I}$ and likewise $\mathbf{B}^\dagger \mathbf{B} = \mathbf{I}$. As our photon, described by vector $\begin{pmatrix} \alpha \\ \beta \end{pmatrix}$, interacts with one of these optical elements, the probability amplitudes will possibly change after the interaction, yet for them to be true probability amplitudes the sum of their absolute squares must always be equal to one, even after transformation. Thankfully, we can prove (very easily) that if a matrix \mathbf{R} is unitary, then it will preserve normalization for any input \vec{v} .

Proof. Suppose \mathbf{R} is unitary. Then consider the transformed vector $\mathbf{R}\vec{v}$. Notice that

$$\begin{aligned} |\mathbf{R}\vec{v}|^2 &= (\mathbf{R}\vec{v})^\dagger (\mathbf{R}\vec{v}) \\ &= \vec{v}^\dagger \mathbf{R}^\dagger \mathbf{R} \vec{v} \\ &= \vec{v}^\dagger \mathbf{I} \vec{v} \\ &= \vec{v}^\dagger \vec{v} \\ &= 1 \end{aligned}$$

Thus we have shown that if a matrix is unitary, it will preserve the normalization property of any vector. Hence we do not need to worry about violating any rules of probabilities when acting these matrices on our state vector. \square

Having found matrix representations for each optical element in the MZI, we could combine these matrices, using matrix multiplication, in order to find one matrix representation for the entire interferometer. One subtle point to notice that will make our computation easier is that the matrix representation for our mirrors is just the identity matrix times minus one. This is because physically speaking, all a mirror does is add a π phase shift to the photon, and in terms of the mathematics involved, this results in multiplying the amplitude of the beam by a factor $e^{i\pi} = -1$. Notice that this phase factor does not affect the probability outcomes since for any probability amplitude γ and any phase ϕ , we have $|e^{i\phi}\gamma|^2 = |\gamma|^2$. Since we will ultimately be using the MZI matrix to calculate the probabilities of various outcomes, and phase factors do not effect these outcomes, we can leave the mirror matrix representation out of the computation and still make accurate predictions. Thus, taking into account the fact that the photon interacts with \mathbf{B}_u and then \mathbf{B}_l , the matrix representation of the MZI is

$$\mathbf{B}_l \mathbf{B}_u = \begin{pmatrix} 0 & -1 \\ 1 & 0 \end{pmatrix}. \quad (2.1.4)$$

If one is still unconvinced that the mirror matrix does not effect the outcomes of the MZI, it is easily shown that

$$\mathbf{B}_l \mathbf{M}_{u,l} \mathbf{B}_u = \begin{pmatrix} 0 & -1 \\ 1 & 0 \end{pmatrix} = \mathbf{B}_l \mathbf{B}_u, \quad (2.1.5)$$

and so the results are equivalent when ignoring the added phase due to the mirrors.

With the matrix representation of the MZI, we can begin computing probability outcomes for the two distinct inputs of the interferometer. From now on, let $\mathbf{Z} = \mathbf{B}_l \mathbf{B}_u$. As well, let detector D_0 be associated with output amplitude β' and let detector D_1 be associated with output amplitude α' . Now we will examine the two possible inputs for the photon.

1. Suppose the input photon beam is $\begin{pmatrix} \alpha \\ \beta \end{pmatrix} = \begin{pmatrix} 1 \\ 0 \end{pmatrix}$ (i.e. the photon is in the upper beam initially). Then the output of the MZI is

$$\begin{pmatrix} \alpha' \\ \beta' \end{pmatrix} = \mathbf{Z} \begin{pmatrix} \alpha \\ \beta \end{pmatrix} = \mathbf{Z} \begin{pmatrix} 1 \\ 0 \end{pmatrix} = \begin{pmatrix} 0 \\ 1 \end{pmatrix}. \quad (2.1.6)$$

Thus, the probability that the photon is detected at D_0 is $P_0 = |\beta'|^2 = 1$, and the probability that the photon is detected at D_1 is $P_1 = |\alpha'|^2 = 0$. Physically, this implies that there is constructive interference in the path that leads to D_0 and destructive interference in the path that leads to D_1 .

2. Now suppose the input photon beam is $\begin{pmatrix} \alpha \\ \beta \end{pmatrix} = \begin{pmatrix} 0 \\ 1 \end{pmatrix}$ (i.e. the photon is in the lower beam initially). Then the output of the MZI is

$$\begin{pmatrix} \alpha' \\ \beta' \end{pmatrix} = \mathbf{Z} \begin{pmatrix} \alpha \\ \beta \end{pmatrix} = \mathbf{Z} \begin{pmatrix} 0 \\ 1 \end{pmatrix} = \begin{pmatrix} 1 \\ 0 \end{pmatrix}. \quad (2.1.7)$$

Thus, the probability that the photon is detected at D_0 is $P_0 = |\beta'|^2 = 0$, and the probability that the photon is detected at D_1 is $P_1 = |\alpha'|^2 = 1$. So, inversely to the first situation, this implies there is destructive interference in the path leading to D_0 and constructive interference in the path leading to D_1 .

These two cases were relatively simple, while conceptually complex, since we did not introduce anything new or unexpected into either beam path (like a phase shifter). The conceptual complexity comes in when we ask ourselves what it means for there to be interference when we are only considering a single photon. One may want to say something such as “Well, the photon must have interfered with itself!”, and while this is a phrase that you may hear in a colloquial setting, the reality is something more nuanced than that. In essence, one can imagine that the the probability amplitudes of each beam differ in phase, and this relative phase difference is what

eventually determines the constructive or destructive interference that occurs at one detector or another. We will not go into a rigorous discussion as to how this all works, but it is important to note the conceptual subtlety in order to avoid developing misconceptions regarding single photon phenomena.

To change things up, let's ask ourselves what would happen to the outcomes if we were to place something into one of the beam paths of the interferometer. Suppose we put a beam block in the lower beam path in the MZI and then carry out the experiment. Then, let the input photon state be $\begin{pmatrix} 1 \\ 0 \end{pmatrix}$. So, after this input photon interacts with the first beam splitter, the probability amplitudes for the two paths are

$$\mathbf{B}_u \begin{pmatrix} 1 \\ 0 \end{pmatrix} = \begin{pmatrix} \frac{1}{\sqrt{2}} \\ \frac{1}{\sqrt{2}} \end{pmatrix}. \quad (2.1.8)$$

From this, what can be gleaned is that there is a probability of $P_{\text{block}} = |\frac{1}{\sqrt{2}}|^2 = \frac{1}{2}$ that the photon hits the beam block and similarly a probability of $P_u = |\frac{1}{\sqrt{2}}|^2 = \frac{1}{2}$ that the photon is in the upper beam after interacting with the first beam splitter. If the photon is in the upper beam, it will continue along this beam path of the interferometer and interact with the second beam splitter. In this case, the input into the second beam splitter is $\begin{pmatrix} \frac{1}{\sqrt{2}} \\ 0 \end{pmatrix}$, where the zero in the second component is because of the fact that the lower beam has been blocked. So, after interacting with the second beamsplitter, the interferometer output is

$$\begin{pmatrix} \alpha' \\ \beta' \end{pmatrix} = \mathbf{B}_l \begin{pmatrix} \frac{1}{\sqrt{2}} \\ 0 \end{pmatrix} = \frac{1}{2} \begin{pmatrix} 1 \\ 1 \end{pmatrix}. \quad (2.1.9)$$

Thus, the outcomes of the interferometer are $P_0 = \frac{1}{4}$, $P_1 = \frac{1}{4}$, and $P_{\text{block}} = \frac{1}{2}$. These results clearly differ from the previous scenario without a beam block, but why is this so? What about placing a beam block along one path changes the outcomes in this way? The fundamental thing that has changed is that introducing a beam block actually removes the possibility for any interference effects to occur at D_0 and D_1 since we have blocked the bottom beam path. Thus if the photon travels along the upper path and reaches the second beam splitter, it is then equally likely to arrive at either detector as we calculated.³

³This example was heavily inspired by Schumacher & Westmoreland. See Schumacher & Westmoreland, *Quantum Processes, Systems, & Information* (Cambridge University Press, 2010), 15-27.

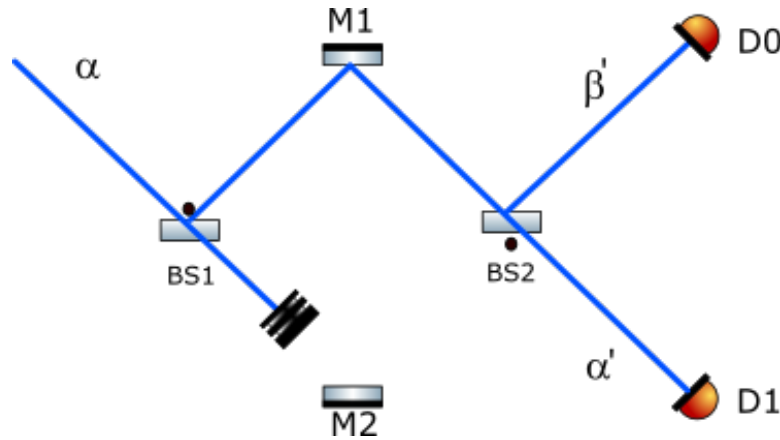


Figure 2.1.2. Mach-Zehnder Interferometer layout with the lower beam blocked. After BS1, there is a 50% chance of the photon being in the upper or lower beam. Since the lower beam never reaches BS2, there are no interference effects to occur, and so there is an equally likely chance of the output photon being in the beam that leads to D_0 or the beam that leads to D_1 .

Amazingly, what this means is that by blocking the lower beam, we have actually increased the chance of detecting a photon at one of the detectors! This example should shed some light on the subtle but critical notion of interference in the context of quantum mechanics and how it conceptually differs from classical mechanics. Although the discussion of measurement theory and interpretation will be reserved for later sections, these types of thought experiments should motivate the reader to leave their notions of classical physics behind as we go deeper into the realm of quantum ways of thinking about reality.

By analyzing the various outcomes from inputting a single photon into a MZI, not only have we revealed some interesting artifacts of quantum theory, but we have also realized that this is just one example of a qubit. In fact, any system that can in some way be broken down into two pieces can be represented by the qubit formalism. Often times these kinds of systems will be called bipartite systems, “two-state” systems, or also “two-level” systems. It just so happens that for the MZI, the two states we are referring to are the two beams of the interferometer. Really, this was clear to us already when we adopted the matrix representation by assuming that the two beam paths act as basis vectors for our qubit vector space (later we will discuss that this is really a Hilbert space). This example of the MZI is particularly interesting in the context of this text as it can be used as just one component of a larger experimental set up that

can be applied to a series of quantum optical experiments. Although this thesis will not go into depth on this topic exactly, the MZI can be used to perform a **Quantum Eraser** experiment; an experiment that probes the curious nature of entanglement, single photon interference, and non-local effects. Moving forward, we will get into a deeper discussion of entanglement, but for now we will focus on another qubit system, the two-level atom, that will reveal even more intricacies of quantum theory.

2.2 Two-level Atoms

In general, atoms of various elements can have certain discrete internal energy levels. While the values of these allowed energy levels vary from atom to atom, what is true for all atoms is the discrete nature of these allowed energy states. For many physical processes, only two energy levels are of particular interest. These are the lowest energy state (or ground state) and one excited state. We can study these types of systems by using a simplified model which only views the two energy levels of particular interest. This is what we will call the *two-level atom*. As we will see, just like the Mach-Zehnder Interferometer (a two-beam interferometer), this type of system can be described using the qubit formalism.

First, let E_0 denote the ground state energy and let E_1 denote the excited state energy. Each discrete energy level corresponds to a quantum state (an eigenstate to be specific) of the atom in question. Thus we may represent these states by kets $|E_0\rangle$ and $|E_1\rangle$ for the ground state and excited state respectively. If one was to measure the energy level of a given two-level atom, it is clear that there are only two distinct possibilities: E_0 or E_1 . Given the distinct quality of these states, we can determine that the quantum states $|E_0\rangle$ and $|E_1\rangle$ satisfy orthonormality:

$$\langle E_0|E_0\rangle = \langle E_1|E_1\rangle = 1, \quad (2.2.1)$$

$$\langle E_0|E_1\rangle = 0. \quad (2.2.2)$$

As in the MZI example, these two states act as an orthonormal vector basis. Because of this, as well as the principle of superposition, an atom can also be in a state that is a superposition

of the allowed energy states. Furthermore, every possible state of the two-level atom can be described by some superposition of these basis elements. Generally speaking, this superposition state takes the form

$$|\phi\rangle = \alpha_0|E_0\rangle + \alpha_1|E_1\rangle \quad (2.2.3)$$

where α_0 and α_1 may be complex, and for some state of the atom $|\psi\rangle$, we can say that $\alpha_k = \langle E_k|\psi\rangle$. A natural question to wonder about is how the state of this type of system may change over time. For instance, if the atom is in the excited state, perhaps as time goes on it will step back down to the ground state. If we recall that the energy of a photon is $E = \hbar\omega$, then we could apply this relation to the two-level atom by saying that if the atom is in a energy state $|E_k\rangle$, then somehow this evolves in time at a frequency $\omega_k = \frac{E_k}{\hbar}$. On a philosophical level, we are not prepared to tackle the question of what it means for a quantum state to evolve over time with some frequency. What we can say however is that the energy itself is **not** changing over time (the energy remains E_k always), rather, something fundamentally quantum mechanical is occurring such that the quantum state of the system evolves in time while the energy level remains constant. The short answer conclusion to this quantum phenomenon is that the complex phase of the state is what is changing in time.

To understand the time evolution of the two-level atom, let's consider the case where the atom is initially in a state with definite energy $|\psi(t=0)\rangle = |E_k\rangle$. Then, at some later time $t = t_f$, the state of the two-level atom is now $|\psi(t_f)\rangle$. By solving the time-dependent Schroedinger Equation via separation of variables, one finds that

$$|\psi(t_f)\rangle = e^{-i\omega_k t_f} |\psi(0)\rangle. \quad (2.2.4)$$

Notice that not only is $|\psi(t_f)\rangle$ also a state with definite energy E_k , but that for a state of this kind, time evolution makes no change at all in terms of calculating the probability of a measurement outcome (this is because $|e^{-i\omega_k t}|^2 = 1$ similarly to the optical phase scenario from the MZI). Because states with definite energies are indistinguishable in time, meaning that at any time the state of the system will have the same energy, we sometimes call them stationary states.

Now that we understand the characteristics of these definite energy states, let us consider the more interesting instance where the state of our atom is in a superposition of these stationary states such as the state $|\phi\rangle$. If we assume for the moment that time evolution of a state acts in a linear manner, we may write that for initial state $|\phi(0)\rangle$, it follows that

$$|\phi(t)\rangle = \alpha_0 e^{-i\omega_0 t} |E_0\rangle + \alpha_1 e^{-i\omega_1 t} |E_1\rangle. \quad (2.2.5)$$

Then, if we consider some other state $|u\rangle$ of the two level atom such that both energy levels are equally likely

$$|u\rangle = \frac{1}{\sqrt{2}} |E_0\rangle + \frac{1}{\sqrt{2}} |E_1\rangle, \quad (2.2.6)$$

the probability amplitude of obtaining the outcome u from a measurement at some time t is

$$\langle u|\phi(t)\rangle = \frac{1}{2}(e^{-i\omega_0 t} + e^{-i\omega_1 t}). \quad (2.2.7)$$

From this, we can find how the probability of measuring outcome u changes over time. Hence

$$\begin{aligned} P_u(t) &= |\langle u|\phi(t)\rangle|^2 \\ &= \langle u|\phi(t)\rangle^* \langle u|\phi(t)\rangle \\ &= \frac{1}{4}(e^{-i\omega_0 t} + e^{-i\omega_1 t})(e^{-i\omega_0 t} + e^{-i\omega_1 t}) \\ &= \frac{1}{4}(2 + e^{i(\omega_1 - \omega_0)t} + e^{-i(\omega_1 - \omega_0)t}) \\ &= \frac{1}{2}(1 + \cos((\omega_1 - \omega_0)t)). \end{aligned} \quad (2.2.8)$$

And so, the probability of the measurement outcome u oscillates between 0 and 1 at a frequency $\omega_1 - \omega_0$.

Behind all of this work is the idea that a linear transformation of a quantum state can describe the time evolution of the said state. We saw that for a stationary state $|E_k\rangle$, the time evolution for any time t is indistinguishable from the initial state $|E_k(0)\rangle$. For a state such as $|\phi\rangle$, we found that when performing this linear transformation, measurement outcomes do in fact change as a function of time. The linear transformation found in this case was a result of solving the time-dependent Schrodinger Equation (although we did not explicitly solve it here). In general, we can call these kinds of linear transformations *operators*. For the time evolution transformation,

which we saw is $e^{i\omega t}$ for some frequency ω , we can say that the time evolution of a state is described by the *time evolution operator* $\mathbf{U}(t)$ which satisfies the two following properties:

1. $\mathbf{U}(t)|E_k\rangle = e^{i\omega_k t}|E_k\rangle$ for some energy state $|E_k\rangle$;
2. $\mathbf{U}(t)$ acts linearly (as we assumed in Eq. 2.2.5).

Having defined the time evolution operator, we can rewrite Eq. 2.2.4 such that

$$|\psi(t)\rangle = \mathbf{U}(t)|\psi(0)\rangle. \quad (2.2.9)$$

The main objective of this section was to introduce the concept of operators and provide a second qubit example to show just how directly the formalism maps onto two seemingly very different physical systems.⁴ In principle, an *operator* is a linear map of a set of vectors independent of any particular vector basis. In this section, we became the most familiar with the time evolution operator, but in principle all observable quantities in quantum mechanics are associated with operators of their own. In the MZI section, for example, the matrices describing the beamsplitter interaction were linear mappings of the basis vectors onto a new state. These are also operators. One other very important set of operators are the *Pauli operators* that are constructed using the qubit basis elements $|0\rangle = \begin{pmatrix} 1 \\ 0 \end{pmatrix}$ and $|1\rangle = \begin{pmatrix} 0 \\ 1 \end{pmatrix}$. In terms of these basis elements, the Pauli operators are

$$\mathbf{X} = |0\rangle\langle 1| + |1\rangle\langle 0| \quad (2.2.10)$$

$$\mathbf{Y} = -i|0\rangle\langle 1| + i|1\rangle\langle 0| \quad (2.2.11)$$

$$\mathbf{Z} = |0\rangle\langle 0| - |1\rangle\langle 1|. \quad (2.2.12)$$

⁴This example was heavily inspired by Schumacher & Westmoreland's discussion of two-level atoms. See Schumacher & Westmoreland, *Quantum Processes, Systems, & Information* (Cambridge University Press, 2010), 36-41.

By computing the outer-products and matrix addition, the Pauli operators have matrix representations called the *Pauli matrices*

$$X = \begin{pmatrix} 0 & 1 \\ 1 & 0 \end{pmatrix} \tag{2.2.13}$$

$$Y = \begin{pmatrix} 0 & -i \\ i & 0 \end{pmatrix} \tag{2.2.14}$$

$$Z = \begin{pmatrix} 1 & 0 \\ 0 & -1 \end{pmatrix}. \tag{2.2.15}$$

This set of operators span the space of observables of the qubit Hilbert space (or 2 dimensional Hilbert space), meaning every observable for a qubit system can be written in terms of Pauli operators and can be used in a variety of situations to measure different components of a quantum observable. As we will see in a later section, they can also be used to determine whether or not certain representations of quantum states are equivalent or not. In general, any measurable quantity in quantum mechanics is called an *observable*, and these observables take the mathematical form of linear operators on a particular Hilbert space of a given quantum system. This is in stark contrast with classical mechanics where measurable quantities take the form of a real-valued function which will determine the measurement outcome over a set of states of the classical system. Examples of such functions are things such as momentum or energy, whereas in quantum mechanics, these functions are replaced with operators. Moving forward, we will utilize the qubit formalism, and what we have learned via studying qubit systems, to explore an even richer and more subtle quantum phenomenon: Entanglement.

3

Entanglement

3.1 Formalism

To study the phenomena of entanglement, or the quantum correlations between spatially separated systems¹, it is necessary to introduce the formalism behind *composite systems*. Put plainly, a composite system is a system composed of two or more distinct subsystems. As an example, imagine having a composite system made up of two distinct subsystems A and B. If we consider the case where each subsystem is prepared independently of the other, such as photons produced via separate processes, the subsystems can be assigned quantum state vectors $|\psi^A\rangle$ and $|\psi^B\rangle$. These state vectors contain all information regarding their respective quantum systems. Furthermore, each state vector belongs to a unique Hilbert space associated with the particular subsystem. For subsystem A, we denote the Hilbert space \mathcal{H}^A , and for subsystem B, we denote the Hilbert space \mathcal{H}^B . To say that each state vector belongs to its respective Hilbert space, we may formally write $|\psi^A\rangle \in \mathcal{H}^A$ and $|\psi^B\rangle \in \mathcal{H}^B$. Note that these Hilbert spaces are just vector spaces with some added structures, and an important property of these vector spaces is that they are closed under linear combination. Being closed under linear combination implies that

¹Freire Junior, *The Quantum Dissidents: Rebuilding the Foundations of Quantum Mechanics (1950-1990)*(Springer, 2015), 235.

for any complex coefficients a and b , it follows that

$$a|\psi_i^A\rangle + b|\psi_j^A\rangle \in \mathcal{H}^A \quad (3.1.1)$$

for all state vectors $|\psi_i^A\rangle, |\psi_j^A\rangle \in \mathcal{H}^A$. The same is true for state vectors in \mathcal{H}^B .

Now that we have laid out the fundamental aspects of Hilbert spaces of a single quantum system, we can consider what it means to describe the Hilbert space of a composite system denoted AB. To construct the Hilbert space of a composite system, we take the tensor product of the individual subsystem Hilbert spaces

$$\mathcal{H}^{AB} = \mathcal{H}^A \otimes \mathcal{H}^B. \quad (3.1.2)$$

The elements of this composite system Hilbert space are called *product vectors*. These product vectors are defined as $|a, b\rangle = |a\rangle \otimes |b\rangle$ such that $|a, b\rangle \in \mathcal{H}^{AB}$ for all $|a\rangle \in \mathcal{H}^A$ and $|b\rangle \in \mathcal{H}^B$. Similarly, the adjoint of the product vector is defined as $\langle a, b| = \langle a| \otimes \langle b|$ such that $\langle a, b| \in \mathcal{H}^{AB}$ for all $\langle a| \in \mathcal{H}^A$ and $\langle b| \in \mathcal{H}^B$. Additionally, the inner product of two product vectors is defined by

$$\langle a_1, b_1|a_2, b_2\rangle = \langle a_1|a_2\rangle\langle b_1|b_2\rangle. \quad (3.1.3)$$

It is also important to note that the tensor product distributes over linear combinations. This is a particularly important note since \mathcal{H}^{AB} is a vector space, meaning it contains arbitrary superpositions of product vectors. Without going through all of the vector space axioms, we may think of \mathcal{H}^{AB} as a closed vector space from this point on. To address a subtle point, one may want to say that the Hilbert space \mathcal{H}^A is a subspace of the composite system Hilbert space \mathcal{H}^{AB} , but recall that \mathcal{H}^{AB} contains *only* product vectors and linear combinations of product vectors. Thus no element of either subsystem Hilbert space could possibly be an element of \mathcal{H}^{AB} .

To better understand the structure of the composite system Hilbert space, it is helpful to know the cardinality of the Hilbert space basis. The number of basis elements of \mathcal{H}^{AB} is called the *dimension* of the vector space, denoted $\dim \mathcal{H}^{AB}$. To see how $\dim \mathcal{H}^{AB}$ depends on the dimension of the subsystem Hilbert spaces, let's suppose $\dim \mathcal{H}^A = d^A$ and $\dim \mathcal{H}^B = d^B$. Then, let $\{e_A\}$ be a basis set for \mathcal{H}^A and let $\{e_B\}$ be a basis set for \mathcal{H}^B . Thus the composite system basis is the

set of all product vectors $\{|e_A, e_B\rangle\} = \{|e_A\rangle \otimes |e_B\rangle\}$. Notice that the set of all possible product vectors contains $d^A d^B$ elements, and so $\dim \mathcal{H}^{AB} = (\dim \mathcal{H}^A)(\dim \mathcal{H}^B) = d^A d^B$.²

What is notable about this result is that the dimension of \mathcal{H}^{AB} , defined using the tensor product, is definitively **larger** than the dimension of a composite classical system which is defined by taking the direct sum (cartesian product) of the state spaces of the classical subsystems. In the classical case, the dimension of the composite state space is the sum of the dimensions of the individual subsystem state spaces as opposed to the product in the quantum composite system case. It is obvious that for any two natural numbers p and q greater than one that $pq \geq p + q$ where the equality only occurs for $p = q = 2$. In short, what this should indicate to us is that when we consider a quantum composite system, we are most often dealing with a larger set of accessible states than if we were considering a classical composite system. By virtue of this, we may expect there to be certain accessible states of the quantum composite system that are never achievable in the classical realm. As we will see, this is in fact the case, and in particular we will see that with this larger set of accessible states comes the possibility for entangled states.

With a bit of mathematical formalism and conceptual understanding of composite systems under our belt we can examine the phenomenon of entanglement. A system with two or more particles (or simply two or more degrees of freedom) is considered to be in an “entangled state” if the state vector, containing all of the information regarding the system, cannot be factored into a product of individual particle state vectors. In this sense, any element of \mathcal{H}^{AB} that **cannot** be written as a product vector is inherently an entangled state. To use a physical example, consider two perfectly correlated photons where the correlation is between the horizontal and vertical polarization states. Using the qubit formalism again, we let the horizontal polarization state (H) be defined as $|H\rangle = \begin{pmatrix} 1 \\ 0 \end{pmatrix}$ and the vertical polarization state (V) be defined as $|V\rangle = \begin{pmatrix} 0 \\ 1 \end{pmatrix}$. Then, the state vector for this perfectly correlated (entangled) state takes the form

$$|\Phi^\pm\rangle = \frac{1}{\sqrt{2}}(|H_1\rangle|H_2\rangle \pm |V_1\rangle|V_2\rangle) \quad (3.1.4)$$

²This informal proof is stated as exercise 6.5 in Schumacher and Westmoreland. See Schumacher & Westmoreland, *Quantum Processes, Systems, & Information* (Cambridge University Press, 2010), 117-120.

for the case of perfect positive correlation, and

$$|\Psi^\pm\rangle = \frac{1}{\sqrt{2}}(|H_1\rangle|V_2\rangle \pm |V_1\rangle|H_2\rangle) \quad (3.1.5)$$

for the case of perfect negative correlation where the subscripts 1 and 2 are to indicate which photon is being regarded. The main feature to be gleaned from these entangled states is the mutual dependence of the results of a polarization measurement. That is, the result of a polarization measurement of one photon immediately implies the polarization of the other photon. For example, suppose we took the case of the positively correlated state. If we were to measure photon 1 to be horizontally polarized in this state, this implies that the polarization state of photon 2 will instantaneously “snap” into the horizontal state as well.

Now that we have demonstrated a mathematical formalism to describe entangled states, let’s begin questioning if things could be otherwise. In particular, given an entangled state, why shouldn’t we be able to describe the state of one particle (or degree of freedom) independently of another one, and what do we learn if we try? To answer this question, let’s consider a general two-level system with basis elements $|\phi_a\rangle$ and $|\phi_b\rangle$, where $\langle\phi_i|\phi_j\rangle = \delta_{ij}$, and form an entangled state using these basis elements. We will show that this entangled state cannot be written as a product vector. This is a completely general case, and so it holds for all types of two level systems (i.e. $|\phi_a\rangle$ could represent vertical polarization and $|\phi_b\rangle$ horizontal, spin up and the other spin down, or could even represent two degrees of freedom of a single particle like in a two dimensional infinite square well). Let one level of the system be denoted by (1) and the other (2). Then, an entangled state of the two-level system is

$$|\psi^{ab}\rangle = \alpha|\phi_a(1)\rangle|\phi_b(2)\rangle + \beta|\phi_b(1)\rangle|\phi_a(2)\rangle \quad (3.1.6)$$

where α and β are coefficients with property $\alpha \neq 0$ and $\beta \neq 0$.

Proof. Let’s assume that it *is* possible to write this entangled state as a product vector. In the $|\phi_a\rangle, |\phi_b\rangle$ basis, we can write two general states as

$$|\psi_r\rangle = c|\phi_a\rangle + d|\phi_b\rangle \quad (3.1.7)$$

and

$$|\psi_s\rangle = e|\phi_a\rangle + f|\phi_b\rangle \quad (3.1.8)$$

where c, d, e and f can be complex. If we take their product, assigning labels (1) and (2) to distinguish between them, we have

$$|\psi_r(1)\rangle|\psi_s(2)\rangle = ce|\phi_a(1)\rangle|\phi_a(2)\rangle + cf|\phi_a(1)\rangle|\phi_b(2)\rangle + de|\phi_b(1)\rangle|\phi_a(2)\rangle + df|\phi_b(1)\rangle|\phi_b(2)\rangle. \quad (3.1.9)$$

If we refer back to Eq. 3.1.6, notice that there is the condition $\alpha \neq 0$ and $\beta \neq 0$. Given this, we cannot retrieve Eq. 3.1.6 from this current expression.

Similarly, we could imagine having an entangled state of the form

$$\gamma|\phi_a(1)\rangle|\phi_b(2)\rangle + \delta|\phi_b(1)\rangle|\phi_a(2)\rangle \quad (3.1.10)$$

where $\gamma \neq 0$ and $\delta \neq 0$. Notice that by the same logic as before, we cannot obtain this entangled state by taking the product of two general states due to the conditions on the complex coefficients. Thus, we have contradicted our hypothesis, and so we conclude that an entangled state cannot be written as a product vector.³ \square

What this proof elucidates for us is that while there may be certain states of a composite system that can be represented by product vectors, for instance the separable solutions of an infinite square well, there are also these allowed entangled states which are clearly of a different variety. This is a core aspect of quantum theory, and thus we can study it deeply as a method of probing the differences between quantum and classical modes of thinking. Studying entanglement for this purpose is not a new realization at all as Einstein, Podolsky and Rosen constructed their famous thought experiment around the subject, which later inspiring John Bell. As the EPR paper began to circulate in 1935, Edwin Schroedinger wrote a letter to Einstein to discuss the recent publication, and in order to describe these states which cannot be factored into product vectors, he coined the term *entanglement*. In his own 1935 paper discussing the topic

³This proof was inspired by an exercise in Chapter 12 of David Griffiths' and Darrel Schroeter's "Introduction to Quantum Mechanics". See Griffiths & Schroeter, *Introduction to Quantum Mechanics* (Cambridge University Press, 2018), 448.

of entanglement, Schroedinger states, "I would not call that one but rather the characteristic trait of quantum mechanics, the one that enforces its entire departure from classical lines of thought."⁴ Thus it seems that entanglement is the perfect playground to study the unique aspects of quantum mechanics which wholly differ from classical ways of describing the universe. Moving forward, we will focus more deeply on these entangled states not only on a theoretical level but on an experimental one as well.

3.2 Examples

The aim of this section will be to address some important conceptual aspects of entanglement not touched upon in the previous material. By way of two different examples, we will see that entanglement is conceptually very subtle. Thus to form a deep understanding of entanglement we must study various entangled systems that highlight these fundamental subtleties. Illuminating these finer points will grant us an amount of clarity on the subject so that moving forward we will be less likely to fall into confusion or misconception.

3.2.1 Basis Dependence

In this example, we will consider one particle confined to two dimensions that is in a "cat state" (or Bell State) shown in Fig. 3.2.1. Most often we think of entanglement to be between two particles, but we can also think of having entanglement between two degrees of freedom of a single particle. In the following example, both cases apply. That is, one could think of the entanglement being between two degrees of freedom of a single particle in two dimensions or equivalently between two particles in one dimension. The difference between these two systems is only semantic in nature, whereas the mathematics is equivalent. So, to describe this entangled state by an analytical formula, one must solve the proper differential equation satisfying certain boundary conditions. This calculation would be tangential to the main point of the example, and since we are more interested in gaining conceptual insight, we will simplify our discussion

⁴E. Schroedinger, *Discussion of Probability Relations between Separated Systems* (1935), 1.

to a qualitatively accurate formula in terms of Gaussian functions⁵. In the (x, y) basis, the wave function takes the form

$$\psi(x, y) = Ae^{-[(y-b)^2+(x-a)^2]/2\sigma^2} + Ae^{-[(y-a)^2+(x-b)^2]/2\sigma^2} \neq \psi(x)\psi(y) \quad (3.2.1)$$

where σ is number whose value is arbitrary in this example, but carries the proper units such that the factor in the exponential is unit-less. Notice that the state of this system cannot be

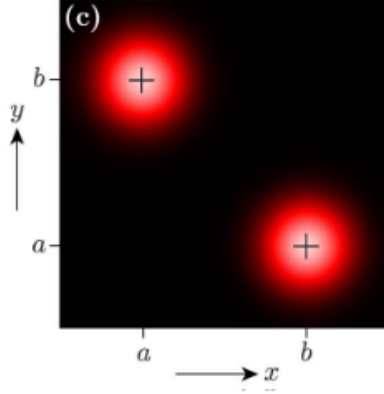


Figure 3.2.1. Graph representing a “cat state” with isolated peaks at (a, b) and (b, a) .

factorized into the product of two wave functions, one for each degree of freedom. Thus, the quantum system described by this wave function is in an entangled state.

Now consider rotating the coordinate axes by 45° counter clock wise. In this new basis, let’s call it the (x', y') basis, the peaks of the two Gaussians align on the x' axis, and thus the wave function takes the form

$$\psi(x', y') = Ae^{-[(x'-b')^2+(y'-a')^2]/2\sigma^2} + Ae^{-[(x'-b')^2+(y'+a')^2]/2\sigma^2} \quad (3.2.2)$$

$$= Ae^{-(x'-b')^2/2\sigma^2} [e^{-(y'+a')^2/2\sigma^2} + e^{-(y'-a')^2/2\sigma^2}] \quad (3.2.3)$$

$$= \psi(x')\psi(y'). \quad (3.2.4)$$

So, in this new basis where both of the Gaussian peaks align with b' , the wave function is separable. Since we proved that entangled states are non-separable, this wave function does not

⁵This example was inspired by an exercise in Daniel Schroeder’s paper “Entanglement isn’t just for spin”.

describe an entangled state. What this example illuminates is that the act of choosing a basis effects the separability or non-separability of the wave function. Furthermore, this means that whenever we are talking about an entangled state we are also implying a choice of basis. This is a very important conceptual point that is often overlooked in many introductions to this topic and can lead to confusion and misconceptions. In short, entanglement is not necessarily an intrinsic property of any particular system, rather it is an artifact of the perspective that one takes when viewing a system. Moving forward, we must always keep in mind that “entanglement is a matter of perspective”.

3.2.2 Polarization Entanglement

This example will examine two polarization entangled photons. In principle, this is simply another example of two particle entanglement, and so everything we have learned up to this point still directly applies. To produce such polarization entangled states, we must first define our polarization basis. For now, let’s stick with the horizontal-vertical polarization basis that we have already used where $|H\rangle = \begin{pmatrix} 1 \\ 0 \end{pmatrix}$ and $|V\rangle = \begin{pmatrix} 0 \\ 1 \end{pmatrix}$. Then, for example, the quantum state of two horizontally polarized photons would be the product state

$$|\psi_i\rangle = |H\rangle_1 \otimes |H\rangle_2 = \begin{pmatrix} 1 \\ 0 \end{pmatrix} \otimes \begin{pmatrix} 1 \\ 0 \end{pmatrix} = \begin{pmatrix} 1 \\ 0 \\ 0 \\ 0 \end{pmatrix}. \quad (3.2.5)$$

Firstly, notice that while this is a composite system, it is not an entangled state. Thus this state vector would describe a system of two photons that were created independently of each other and have no interaction between them. So, if we wanted to work with a system of two photons whose polarization states are entangled, some kind of interaction will need to occur between them to generate such correlations in their polarizations. This exact scenario of generating polarization entangled photons will serve as the foundation for testing Bell’s Theorem, but until that point, we will try to gain some familiarity with polarized light in the context of quantum mechanics in general.

When light is sent through a polarizer, the state of the light is projected onto the polarizers transmission axis. If we define the angle of the transmission axis to be some angle θ relative to the horizontal axis, then the polarizer eigenstates of transmission are

$$|\theta\rangle = \begin{pmatrix} \cos \theta \\ \sin \theta \end{pmatrix}. \quad (3.2.6)$$

Another way of putting it is that when the light is introduced to the polarizer, the state of the light is projected onto the polarizer eigenstates of transmission. Clearly, the amount of light projected onto each individual eigenstate depends on the angle θ and the initial polarization state of the light. So, if we were to take our two photon state and send each photon through their own polarizer, one set to θ_1 and the other θ_2 , then both photons are projected onto the polarizer eigenstates such that the two-photon polarization state vector takes the form

$$|\psi_p\rangle = \begin{pmatrix} \cos \theta_1 \\ \sin \theta_1 \end{pmatrix} \otimes \begin{pmatrix} \cos \theta_2 \\ \sin \theta_2 \end{pmatrix} = \begin{pmatrix} \cos \theta_1 \cos \theta_2 \\ \cos \theta_1 \sin \theta_2 \\ \sin \theta_1 \cos \theta_2 \\ \sin \theta_1 \sin \theta_2 \end{pmatrix}. \quad (3.2.7)$$

Having found the general expression for the quantum state of two photons projected onto the polarizer eigenstates of transmission, we can ask what the probability is of detecting both photons past their respective polarizers. If we input state $|\psi_i\rangle$ into the polarizers, then the probability of a joint detection of the photons being in state $|\psi_p\rangle$ is

$$P_p = |\langle \psi_p | \psi_i \rangle|^2 = |\cos \theta_1 \cos \theta_2|^2. \quad (3.2.8)$$

To check that this result is reflective of physical reality, we can consider a couple of cases where we know whether or not the two photons should be transmitted or not. For the first case, let $\theta_1 = \theta_2 = 0^\circ$ meaning both polarizers are set to transmit horizontally polarized light. Thus, the probability of joint detection is $P_0 = |\cos 0 \cos 0|^2 = 1$. As expected, when both polarizers have transmission axes set to horizontal, we expect to detect both horizontally polarized photons every single time. By the same logic, one can quickly see that when both polarizers are set to 90° , the probability of a joint detection of two horizontally polarized input photons is zero. Again, this is the expected result since we expect a horizontally polarized photon to **never** transmit through

a vertically oriented polarizer. Clearly, these were the two extreme cases. As for probabilities between 0 and 1, one can see that these instances only occur when the transmission axis of either polarizer is set to some angle between these two extremes.

Now that we have unpacked the concept of polarization measurements for two photon systems, let us consider how we may generate photon pairs that are polarization entangled. In order to generate this kind of system, we must have some kind of physical process that will output two indistinguishable photons which are both in a superposition of polarization states. One clever physical process that does this involves two down-converting crystals that exhibit Type 1 Spontaneous Parametric Down-Conversion (SPDC) under certain “phase matching” conditions. Later chapters go into depth regarding the phenomena of SPDC and phase matching, but for now all that we need to know here is that when you input one photon polarization state into the down-converting crystal, two correlated photon pairs are generated with orthogonal polarizations to the input photon. In this situation, we would like to create a whole bunch of photon pairs where some are vertically polarized and others are horizontally polarized. To do this, we can imagine placing thin two down-converting crystals next to each other (face to face) but with one crystal rotated 90° relative to the other. Then, imagine sending in a beam that is polarized at 45° relative to the horizontal axis. If the pair of crystals is oriented properly relative to the input beam polarization, we find that the vertical component of the input polarization will generate horizontally polarized pairs in one crystal, and in the horizontal component of the input polarization will generate vertically polarized pairs in the other crystal.

In general, we have just created a system that will generate a mixture of pairs where some are vertically polarized and others are horizontally polarized. This is interesting and can even be useful in certain situations, but it is not an entangled system. To make these photon pairs exhibit polarization entanglement, we must have some method of making the creation of down-converted pairs indistinguishable. That is, we must generate these pairs via some process such that the apparatus cannot distinguish which crystal the photon pair was created in.

There is a two part trick to make the paths of the photon pairs indistinguishable: Firstly, if the thickness of the crystal is smaller than the beam width (which can easily be found with a beam profiler or calculated by treating the beam as a Gaussian), then the creation of photon pairs will be spatially indistinguishable. Secondly, there will be a time delay between the creation of photon pairs in either crystal due to the difference in velocity of light in the crystal medium as a function of wavelength. That is, the pump photon will spend a different amount of time in the first crystal than a down converted photon will, and this is due to the difference in wavelength (and thus wave speed in the crystal). This time delay makes the paths of the photons distinguishable, but using a compensating crystal to delay one of the components of the inputs beam's polarization before interacting with the down-converting crystal, this time delay can be done away with making the photon pairs indistinguishable once again.⁶ Once the paths have become indistinguishable, we have successfully created photon pairs in a state that is a superposition of the two possible polarizations:

$$|\Phi\rangle = \frac{1}{\sqrt{2}}(|H\rangle_1|H\rangle_2 + |V\rangle_1|V\rangle_2 e^{i\delta}). \quad (3.2.9)$$

Here, δ acts as a phase between the two possible measurement outcomes, and in principle this phase influences the correlation between photons. For the sake of simplicity, and without losing the core of the argument, we shall let $\delta = 0$ giving us a maximally correlated state. Then Eq. 3.2.9 takes the form

$$|\Phi^+\rangle = \frac{1}{\sqrt{2}}(|H\rangle_1|H\rangle_2 + |V\rangle_1|V\rangle_2) = \frac{1}{\sqrt{2}} \begin{pmatrix} 1 \\ 0 \\ 0 \\ 1 \end{pmatrix} \quad (3.2.10)$$

where the “+” is to indicate that this is a state with maximal positive correlation.

As a quick aside, notice that we chose to write this state in the horizontal-vertical basis, and we found that in this basis our system is in an entangled state. What would happen if we wrote this state in another basis? To see this, let us define the diagonal-antidiagonal polarization basis

⁶Refer to Appendix B for a derivation of the compensating crystal thickness needed to compensate this time delay.

as

$$|D\rangle = \frac{1}{\sqrt{2}}(|H\rangle + |V\rangle) \quad (3.2.11)$$

$$|A\rangle = \frac{1}{\sqrt{2}}(-|H\rangle + |V\rangle) \quad (3.2.12)$$

Then, we may write $|H\rangle$ and $|V\rangle$ in terms of $|D\rangle$ and $|A\rangle$ such that $|H\rangle = \frac{1}{\sqrt{2}}(|D\rangle - |A\rangle)$ and $|V\rangle = \frac{1}{\sqrt{2}}(|D\rangle + |A\rangle)$. By making these substitutions in Eq. 3.2.10 and simplifying, notice

$$|\Phi^+\rangle = \frac{1}{\sqrt{2}}(|D\rangle_1|D\rangle_2 + |A\rangle_1|A\rangle_2). \quad (3.2.13)$$

So, in contrast to section 3.2.1, we see that this change of basis results in another entangled state in which the photons are in a superposition of states that are parallel to each other. Having written the entangled state in two bases, it would be natural to ask what the probability that a photon in state $|\Phi^+\rangle$ is measured to be in a state $|\psi_p\rangle$. Notice

$$\begin{aligned} P_{\psi_p} &= |\langle\psi_p|\Phi^+\rangle|^2 \\ &= \frac{1}{2}|\cos\theta_1\cos\theta_2 + \sin\theta_1\sin\theta_2|^2 \\ &= \frac{1}{2}\cos^2(\theta_1 - \theta_2). \end{aligned} \quad (3.2.14)$$

So, we get the maximum probability when the two angles are the same. Since we did not pick a particular polarization basis to make this measurement in, rather we just left θ_1 and θ_2 arbitrary, we can infer from the fact that the probability is maximal for equal angles that all photon pairs in state $|\Phi^+\rangle$ are parallel in *any* polarization basis.

Having found the initial entangled state by arguing for a physical phenomena rather than providing a rigorous derivation, it would seem legitimate to be a bit skeptical of this result. Someone who remains unconvinced that the physical process described will truly produce polarization entangled photons may argue that instead this physical process just creates vertically polarized pairs half the time and horizontally polarized pairs the other half of the time. This would be a mixed state rather than an entangled state. We must be able to distinguish between the case of a mixed state and an entangled state to show that in practice, the physical system at hand truly generates entangled photons and not just a mixed state. One way of trying to

answer this question mathematically is by examining the density matrix of the entangled state $|\Psi^+\rangle$ and comparing it to the density matrix of the mixed state. The density matrix is defined as the outer product of the state with itself such that

$$\rho_{\Phi^+} = |\Phi^+\rangle\langle\Phi^+| = \frac{1}{2} \begin{pmatrix} 1 & 0 & 0 & 1 \\ 0 & 0 & 0 & 0 \\ 0 & 0 & 0 & 0 \\ 1 & 0 & 0 & 1 \end{pmatrix}. \quad (3.2.15)$$

If we were to consider the mixed state where half of the photons are horizontally polarized and the other half are vertically polarized, we may represent this as a linear combination of the density matrices for the two pure states. Thus

$$\rho_{\text{mix}} = \frac{1}{2}|H\rangle_1|H\rangle_2\langle H|_1\langle H|_2 + \frac{1}{2}|V\rangle_1|V\rangle_2\langle V|_1\langle V|_2 = \frac{1}{2} \begin{pmatrix} 1 & 0 & 0 & 0 \\ 0 & 0 & 0 & 0 \\ 0 & 0 & 0 & 0 \\ 0 & 0 & 0 & 1 \end{pmatrix}. \quad (3.2.16)$$

By a simple comparison between the representations of the mixed state and the density matrix of the entangled state, it is obvious that these two representations differ. This should be the first indication, and a good one, that these two physical scenarios are truly distinct from each other. Another way to see that these states differ is by finding the probability that a mixed state will be measured in state $|\psi_p\rangle$. If we consider our mixed state to be represented by $|\phi\rangle$, then the probability of detection is given by

$$P_{\text{mix}} = |\langle\psi_p|\phi\rangle|^2 = \text{Tr}(\rho_{\psi_p}\rho_{\text{mix}}). \quad (3.2.17)$$

By taking the outer product of $|\psi_p\rangle$ with itself, and only looking at the diagonal entries since we will be taking the matrix product with ρ_{mix} which only has non-zero entries on the diagonal, notice

$$\rho_{\psi_p} = \begin{pmatrix} \cos^2\theta_1 \cos^2\theta_2 & \cdot & \cdot & \cdot \\ \cdot & \cos^2\theta_1 \sin^2\theta_2 & \cdot & \cdot \\ \cdot & \cdot & \sin^2\theta_1 \cos^2\theta_2 & \cdot \\ \cdot & \cdot & \cdot & \sin^2\theta_1 \sin^2\theta_2 \end{pmatrix}. \quad (3.2.18)$$

Then, through some basic matrix multiplication and taking the trace, which amounts to summing the diagonal entries, we find that

$$P_{\text{mix}} = \text{Tr}(\rho_{\psi_p}\rho_{\text{mix}}) = \frac{1}{2} \cos^2\theta_1 \cos^2\theta_2 + \frac{1}{2} \sin^2\theta_1 \sin^2\theta_2. \quad (3.2.19)$$

Not only does this result clearly differ in functional form from Eq. 3.2.14, but these probabilities are quantities accessible to us in a laboratory setting. Thus we can use these two results to test, in a physical setting, whether or not the down-conversion process described above truly creates polarization entangled pairs.

One other way of seeing the mathematical difference between these two scenarios is by way of a slightly obscure method. Although obscure and not as accessible experimentally, this method does reveal something interesting about these two different cases. If we refer back to the Pauli operators from the section on two-level atoms, we can recall that these operators span the entire space of 2×2 matrix observables. Clearly, these density matrices do not have dimension equal to 2 (the dimension is in fact 4), and so we run into an issue when trying to apply to Pauli operators. In the qubit case, we know that the Hilbert space for a qubit has dimension 2. When considering mixed and entangled states of two qubits, we can see that the Hilbert space for this composite system is the tensor product of two individual qubit Hilbert spaces. For this reason, the Hilbert space governing all possible two-qubit states has dimension equal to four. In order to construct operators that we can act on our entangled and mixed states, we may take the tensor product of the Pauli matrices with themselves. If we only consider the Pauli matrices X and Z , notice

$$V = X \otimes X = \begin{pmatrix} 0X & 1X \\ 1X & 0X \end{pmatrix} = \begin{pmatrix} 0 & 0 & 0 & 1 \\ 0 & 0 & 1 & 0 \\ 0 & 1 & 0 & 0 \\ 1 & 0 & 0 & 0 \end{pmatrix} \quad (3.2.20)$$

and

$$W = Z \otimes Z = \begin{pmatrix} 1Z & 0X \\ 0Z & -1Z \end{pmatrix} = \begin{pmatrix} 1 & 0 & 0 & 0 \\ 0 & -1 & 0 & 0 \\ 0 & 0 & -1 & 0 \\ 0 & 0 & 0 & 1 \end{pmatrix}. \quad (3.2.21)$$

By computing the expectation value of these new operators for the entangled state $|\Phi^+\rangle$, we find that

$$\langle V \rangle_{\Phi^+} = \langle \Phi^+ | V | \Phi^+ \rangle = 1 \quad (3.2.22)$$

$$\langle W \rangle_{\Phi^+} = \langle \Phi^+ | W | \Phi^+ \rangle = 1. \quad (3.2.23)$$

Then, by computing the expectation value of these operators for the mixed state ρ_{mix} , notice

$$\langle V \rangle_{\rho_{\text{mix}}} = \text{Tr}(\rho_{\text{mix}} V) = 0 \quad (3.2.24)$$

$$\langle W \rangle_{\rho_{\text{mix}}} = \text{Tr}(\rho_{\text{mix}} W) = 1. \quad (3.2.25)$$

These are very interesting results! Notice how $\langle W \rangle_{\Phi^+} = \langle W \rangle_{\rho_{\text{mix}}}$ but $\langle V \rangle_{\Phi^+} \neq \langle V \rangle_{\rho_{\text{mix}}}$. So, in this particular case we see that the mixed state and entangled state may act similarly in certain ways, yet clearly not in every way. This is just further indication that these states are truly describing two different physical circumstances.

4

Generating Down-Converted Photon Pairs

While studying the mathematics underlying entangled systems can be quite rich and satisfying on its own, it would also be illuminating to be able to observe entangled systems in a laboratory setting. This chapter presents the theoretical background behind the particular down-conversion process being exploited in order to create down-converted pairs as well as the necessary optical alignment procedure. In the end of this chapter, there is a presentation of the experimental procedure for verifying the production and detection of these down-converted photon pairs.

4.1 Spontaneous Parametric Down Conversion

The primary physical phenomena being exploited in order to generate down-converted pairs is Type-I Spontaneous Parametric Down-Conversion (SPDC). Down-conversion is a non-linear dynamical process that occurs between the atoms in the beta barium borate (BBO) crystal and incident photons. In Type-I SPDC, the down-converted photons have the same polarization, which is orthogonal to the input photon polarization. To build a theoretical understanding of this process, consider a photon entering the BBO crystal. We will call this input photon the *pump photon*. As a pump photon with energy E_0 enters the crystal, it is spontaneously annihilated and two more photons are emitted with energies E_1 and E_2 . We will call these the *signal* and *idler* photons, or together we refer to them as a down-converted pair. By the conservation of

energy

$$E_0 = E_1 + E_2, \quad (4.1.1)$$

or in terms of the wavelength in vacuum since $E = \frac{hc}{\lambda}$,

$$\frac{1}{\lambda_0} = \frac{1}{\lambda_1} + \frac{1}{\lambda_2}. \quad (4.1.2)$$

As well, the momentum must be conserved in order to produce down-converted photons. Thus

$$\vec{p}_0 = \vec{p}_1 + \vec{p}_2. \quad (4.1.3)$$

These equations regarding the conservation of energy and momentum are known as *phase-matching* conditions. As we will see, the phase matching conditions are only met by certain combinations of wavelengths, and these wavelengths depend on the indices of refraction of the BBO. Down-converted photons are only produced when these conditions are met. A visual representation of the phase-matching conditions can be seen in Fig. 4.1.1.

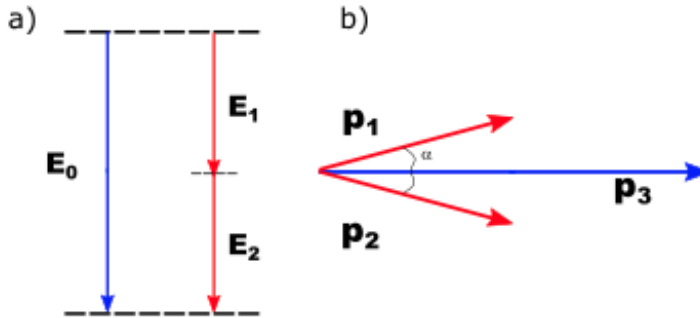


Figure 4.1.1. Visual representation of energy and momentum conservation in the context of Spontaneous Parametric Down-Conversion. The blue lines indicate the energy and momentum of the pump photon while the red lines indicate the energy and momentum of the signal and idler photons.

When light travels from vacuum to some new medium, its wavelength changes due to refraction. This is accounted for by the index of refraction of the medium n such that $\lambda = \frac{n}{\lambda_0}$, where λ_0 is the wavelength in vacuum. If we consider a coordinate system such as the one shown in Fig. 4.1.2, we can break down the photon momentum into components. It follows from the figure that there is no input momentum in the y -direction, thus

$$p_{0y} = p_{1y} + p_{2y} = 0. \quad (4.1.4)$$

Recall $p = \frac{2\pi\hbar n}{\lambda}$, and so this equation becomes

$$\frac{n_1}{\lambda_1} \sin \theta_1 - \frac{n_2}{\lambda_2} \sin \theta_2 = 0. \quad (4.1.5)$$

This holds assuming the photons are not degenerate. Notice from this relation that it is possible for the two photons to be emitted at different angles so long as they have different energies (and thus momenta). For conservation of momentum along the direction of the pump beam

$$p_{0x} = p_{1x} + p_{2x} = p \quad (4.1.6)$$

or,

$$\frac{n_0}{\lambda_p} = \frac{n_1}{\lambda_1} \cos \theta_1 + \frac{n_2}{\lambda_2} \cos \theta_2. \quad (4.1.7)$$

If the two down converted photons have the same wavelength ($\lambda_1 = \lambda_2$), as is the desired case in our set up, then by Eq. 4.1.5, it follows that $\theta_1 = \theta_2$. Now consider the case when $\lambda_1 = \lambda_2 = 2\lambda_p$. Then, Eq. 4.1.7 reduces to

$$n_0 = n_1 \cos \theta_1. \quad (4.1.8)$$

And if we consider the special case of collinear emission ($\theta_1 = \theta_2 = 0$), notice that we get back to the expected result

$$n_0 = n_1, \quad (4.1.9)$$

which confirms that collinear emission is a result of the index of refraction remaining constant as the light changes media.

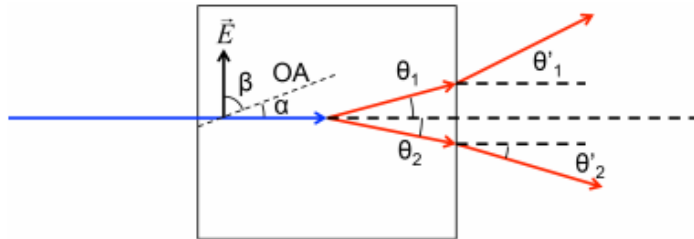


Figure 4.1.2. Diagram of the BBO crystal. The red arrows indicate the signal and idler photon directions and the blue arrow indicates the pump photon input direction. The y-coordinate direction is upwards, and the x-coordinate direction is horizontal to the right.

In a birefringent medium like a BBO crystal, the index of refraction depends on the polarization of the input electric field. If the input electric field polarization is orthogonal to the optic axis of the crystal, the index of refraction is called “ordinary” and is denoted n_o . If the input electric field polarization is parallel to the optic axis, the index of refraction is then referred to as “extraordinary” and is denoted n_e . The value of these two indices for the BBO crystal depend on the wavelength of the input electric field and are given empirically by¹:

$$n_e = 2.3753 + \frac{0.01224}{(\lambda/1\mu m)^2 - 0.01667} - 0.01516(\lambda/1\mu m)^2)^{1/2} \quad (4.1.10)$$

and

$$n_o = 2.7359 + \frac{0.01878}{(\lambda/1\mu m)^2 - 0.01822} - 0.01354(\lambda/1\mu m)^2)^{1/2} \quad (4.1.11)$$

In the case of a 405nm pump beam with the direction of propagation normal to the crystal surface, the indices are $n_{e0} = 1.5671$ and $n_{o0} = 1.6919$. For the case of the down-converted photons at 810nm, the indices are $n_{e1} = 1.5442$ and $n_{o1} = 1.6603$. We use the first case to account for the refraction that occurs during the transition from air to the crystal medium, and the second to account for the transition from the crystal back to the air.

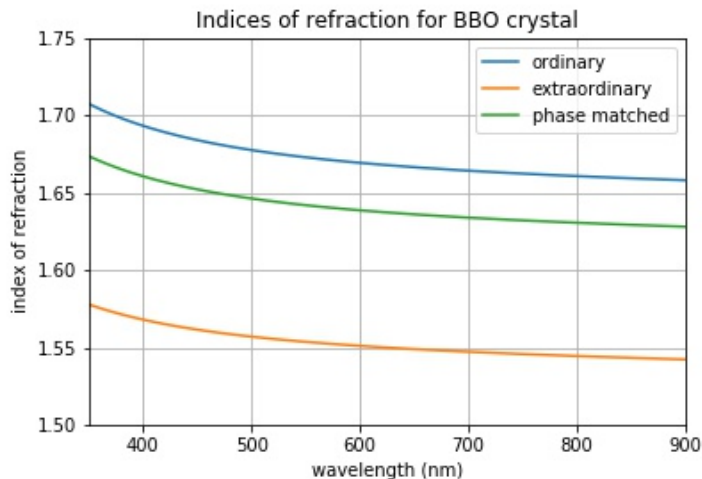


Figure 4.1.3. This graph shows the different indices of refraction of the BBO as a function of wavelength.

¹These empirical constants can vary slightly in value, but these were taken from Enrique Galvez’s lab manual that can be found on his website cited in the bibliography

It is possible to tune the extraordinary index of refraction by adjusting the angle β between the input polarization and the optic axis. This can also be expressed this in terms of the angle which the input beam makes with optic axis denoted $\alpha = \pi - \beta$. Knowing that the velocity of light in a medium depends on the index of refraction, we may be able to find a relationship between the index of refraction and the angle α . Thus, we can find an equation describing how the index of refraction changes as the angle between the input polarization and optic axis change. Recall that $v_{\text{vac}} = c$ and $v_{\text{med}} = \frac{c}{n}$. So, in terms of components, the velocity of light in the crystal is

$$v_{\text{med}} = \left| \frac{v_{\text{vac}}}{n} \right| \quad (4.1.12)$$

$$= \sqrt{\frac{c^2 \cos^2 \alpha}{n_o^2} + \frac{c^2 \sin^2 \alpha}{n_e^2}} \quad (4.1.13)$$

$$= c \sqrt{\frac{\cos^2 \alpha}{n_o^2} + \frac{\sin^2 \alpha}{n_e^2}} \quad (4.1.14)$$

$$= \frac{c}{n} \quad (4.1.15)$$

Solving for n in terms of n_o , n_e and α gives us the index of refraction depending on how parallel the input polarization is to the optic axis. Thus we give it the subscripts $n_{e,\alpha}$ and conclude

$$n_{e,\alpha} = \left(\frac{\cos^2 \alpha}{n_o^2} + \frac{\sin^2 \alpha}{n_e^2} \right)^{-1/2}. \quad (4.1.16)$$

With this, we can determine the angle at which down-converted pairs are generated within the crystal. Using Eqn. 4.1.8 and solving for θ_1 in this particular case

$$\theta_1 = \cos^{-1} \left(\frac{n_{e,\alpha}}{n_{o1}} \right). \quad (4.1.17)$$

To get a numerical value for θ_1 , we must have some values for $n_{e,\alpha}$ and n_o . That is to say, we must decide two parameters of our experiment: the wavelength of the down-converted photons and the angle between the optic axis and the polarization of the input electric field. Let the wavelength of the refracted light be 810nm and let the angle between the optic axis of the crystal and the input polarization be 29.95° (the significance of these values will become clear later on). Then $n_{e,\alpha} = 1.6594$ and by recalling the value for n_{o1} , we find that $\theta_1 = 1.8^\circ$. Thus, to satisfy the conservation of momentum, we conclude that one down-converted photon is generated at an

angle $+1.8^\circ$ and the other at an angle -1.8° . This can be visualized as in Fig. 4.1.2. Then, the down-converted pairs are refracted as they exit the crystal, and so recalling Snell's Law

$$n_{\text{air}} \sin \theta'_1 = n_{o1} \sin \theta_1 \quad (4.1.18)$$

one can apply this, knowing that $n_{\text{air}} = 1$, to find that one down-converted photon exits the crystal at an angle

$$\theta'_1 = \sin^{-1} (n_{o1} \sin \theta_1). \quad (4.1.19)$$

For this case, we find that $\theta'_1 = 3.1^\circ$. And again, the down-converted pairs must satisfy the conservation of momentum, and so as one is refracted by an angle $+3.1^\circ$, the other must be refracted by an angle -3.1° . So, we have found that for the case of 810nm down-converted photons with $\alpha = 29.95^\circ$, the down converted pairs will be separated by an angle 6.2° as they exit the crystal. This value is crucial in determining the placement of our detection apparatus. As an aside, notice that the indices of refraction are dependent on the wavelength entering the crystal. Because of this, the angles of refraction will also be dependent on the wavelength of the input light. In the following experiments however, we will always be using the same wavelength laser, 405nm, and so θ'_1 will remain constant.

4.2 Optical Alignment Procedure

This section is concerned with the placement and alignment of the optical components needed to generate down-converted pairs. All of the optical components needed for this experiment are as follows.

1. HeNe laser as alignment (pilot) beam.
2. GaN diode laser (405nm, $>20\text{mW}$) for generating down-converted pairs.
3. Beta Barium Borate (BBO) crystal for generating down-converted pairs.
4. Four mounted mirrors (two for each laser) used for alignment of the beams.

5. One flipper mirror used for HeNe alignment.
6. Two iris' for alignment.
7. Two mounted fiber collimators.
8. 810nm line filters to eliminate any extraneous light from entering the fiber collimators.

In the previous section, we found that for a pump photon at 405nm, we expect two down-converted photons of wavelength 810nm to be emitted with an angle of 6.2° separating them. Given this information, we can use some simple trigonometry to determine where to best place fiber collimators to capture these down-converted pairs. Let us assume we will place the fiber collimators one meter from the crystal (the point where the pairs are created). Knowing the angle of separation between the down-converted pairs, we determine how far apart to place the our fiber collimators by taking the tangent of this angle. Doing so, we find that $\tan(6.2^\circ) = d = 0.108\text{m} = 10.8\text{cm}$. Thus by placing the fiber collimators one meter away from the crystal, we find that the separation between collimators should be 10.8cm.

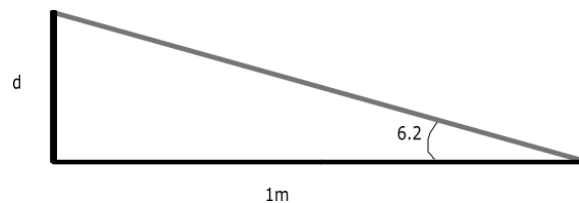


Figure 4.2.1. Triangle representing the two paths taken by the down-converted photons where d refers to the distance between fiber collimators necessary to capture these photons and direct them towards their respective Single Photon Counting Modules.

Now we will go into the step by step procedure for aligning all of the necessary optics.

Laser Alignment: We start by dealing with the HeNe laser since this is what will be used to align all of the fiber collimators. The alignment for the GaN laser is identical, and thus the following procedure should be carried out for both lasers. We will refer to the HeNe laser as the “alignment beam”. Before beginning to set things up, one must decide the height above the table to place the laser. This choice is usually determined by the size of the hardware available, and this decision will subsequently determine the height of other optical components as we

intend for the laser to travel in a plane parallel to the optical table. Here, we placed the laser approximately 4.375in from the surface of the table. The objective here is to, using two mirrors, make the alignment beam to travel along a plane which is parallel to the optical table and parallel to a line of holes on the optical table.

1. Mount HeNe laser securely to the table and place mirrors M1 and M2 as shown in Fig. 4.2.2. At this point, the beam will not be parallel to the table or parallel to the rows of holes on the table.
2. Mount two iris' such that their pupils are at the desired height above the table. Choose a row of holes on the table to make the alignment beam parallel to. This row of holes will need to roughly intersect the placement of M2. After choosing a row, place two pairs of bolts adjacent to each other on this row. One pair should be near M2 and the other pair should be farther away from M2 (about 1m away from M2 works well). With the pupils mostly closed while still letting some light through, place the base of the mounted iris' against the pairs of bolts (one pair near M2 and the other about 1m away). By a rough estimation (use your eyes), check to make sure that there is a straight line that connects the pupils and the surface of M2. This alignment procedure will not work otherwise. **Do not do this with the laser on! Never get your eye near a laser beam!**
3. With the iris' in place, use the adjustment knobs on M1 to send the beam through the near iris. Then, open the nearer iris and use the adjustment knobs on M2 to send the beam through the further iris. Iterate this process as many times as needed (likely only three or four times if done correctly) until no more adjustment is needed to send the beam cleanly through both iris'. Once this is achieved, we can be certain that the beam travels along a plane that is parallel to the table and along a straight line parallel to the rows of holes on the table. If this procedure did not work, go back and check the relative positions of M2 and the row of holes where the iris' are placed.

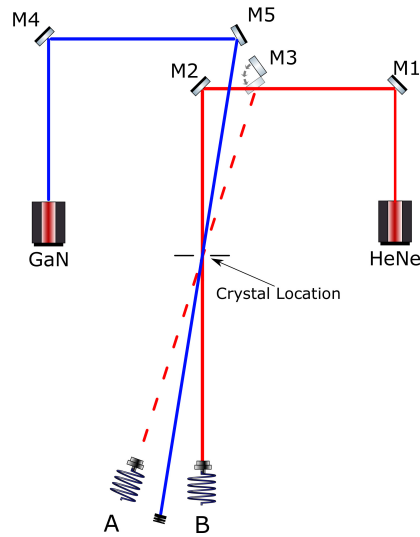


Figure 4.2.2. Down-Conversion experimental apparatus. The red lines indicate the HeNe laser, and the blue indicates the GaN laser. In this diagram, the BBO crystal is not in place, but the expected location is indicated as we need it to predict the fiber collimator placement.

Something to consider when putting this together is the distance between the optics as well as the distance from the edge of the table to the beam that we just aligned. To avoid running into problems when placing more hardware later on, it is advisable to place M1 and M2 at least 6in away from any edge of the table, and the beam reflected from M2 that is now parallel to the rows of holes should be roughly 12in away from the nearest edge of the table. The same process should be carried out for the GaN laser using M4 and M5. In the end, this procedure should give a set-up that is beginning to resemble Fig. 4.2.2.

4.2.1 *Generating and Detecting Down Converted Photons*

With the optical alignment procedure complete, we can place the BBO crystal and begin the alignment of the crystal in order to maximize the detection of down-converted pairs. The procedure for generating and detecting down-converted photon pairs is as follows.

1. **Place The Crystal:** Mount the BBO crystal in a rotating mount to allow for tuning of the angle between the optic axis and the input polarization. Place the crystal in the beam path, after the alignment mirrors, 1m from where the fiber collimators will be placed. In the section on SPDC, we found that an angle of 29.95° between the optic axis of the BBO and the input polarization gave the desired phase matching conditions. Because these BBO crystals are often used for the purpose of generating down-converted pairs, many BBO crystals are already mounted such that the 0° mark is already 29.95° away from the optic axis.
2. **See Photons:** The down-converted photons are collimated into a fiber optic cable which allow them to travel into individual Single Photon Counting Modules (SPCM's). When a photon is detected, the SPCM's generate consistent electronic pulses that trigger the digitizer to convert the analog electronic signal into digital time-stamped data. To check that the SPCM's are sending pulses with the proper temporal length and amplitude to trigger the digitizer, plug the output of the SPCM's into an oscilloscope and examine the signal. The pulses should be roughly 20ns long and 0.2V in amplitude. This will lower the possibility of saturating the digitizer detectors.
3. **Maximize Counts:** Having ensured that the SPCM's output the desired electromagnetic pulse, the next step is to use the digitizer along with the data acquisition software CoMPASS by CAEN to begin counting the down-converted photons being detected by each SPCM. Note that it may be optimal to work in complete darkness if you do not have a dark box for all of the optics and SPCM's. We opted to work in complete darkness except for the computer screen facing away from the fiber collimators. Once everything is set up properly and all devices are on, the first line of action should be to rotate the crystal orientation and see how that effects the singles and coincidence counts on each detector. The goal is to find the orientation of the crystal that gives the largest number of coincidences. Assuming that the alignment of the optics and fiber optic cables has been done well, you should be seeing some counts at this point. If not, unscrew the fiber cables

from the SPCM's and use the red alignment laser to ensure that the fiber collimators are aligned such that they allow as much light as possible through them. A photodetector and oscilloscope may be useful for this. After rotating the crystal to maximize counts and possibly checking the fiber alignment, the next step towards maximizing counts should be to use the fine adjustment knobs on the fiber collimator mounts. Note that these can be quite sensitive, and so one should be **very** patient during this entire process. One should expect to go over this process a few times to make sure they have optimally aligned the crystal and fiber collimators. When measuring singles counts and coincidences, the counts per second can vary a lot depending on the power of the laser being used as well as the other optical elements. In the end however, one should expect to be getting on the order of tens of thousands of singles counts per second on each detector.

4. Check Measurements: To know if these counts are true down-conversions from the crystal and not just ambient noise signals, we must check that the coincidence counts of the two detectors are larger than the accidental coincidences. That is to say, even without the down converted photons, the data acquisition system will still detect some amount of accidental coincidences since there is still some chance of photons arriving at the detectors within the set time interval even without down-converted pairs present. This number of accidental coincidences is given by

$$N_{acc} = N_1 N_2 \Delta T \quad (4.2.1)$$

where the singles counts per second are N_1 and N_2 , and ΔT is the coincidence window set by the digitizer. The data acquisition software² limits the possible coincidence windows to multiples of eight, but in the end we will be doing our own coincidence counting using a MATLAB code. For now though, just to check that we are detecting down-converted photons, a suitable coincidence window is 32ns. With proper alignment, we should expect coincidences counts per second that are as high as 10% of the singles counts per second.

This means, for example, that if both detectors registered approximately 20,000 singles

²For more information regarding the data acquisition software, refer to Appendix A.

counts per second, then we should expect to detect about 2000 coincidences per second at most. In our own experimental process, the maximal coincidences per second achieved was 8.5% of the singles counts per second.

5

Hanbury Brown-Twiss Experiment

Having confirmed the functionality of the experimental set-up described in the previous chapter, we can make some additional adjustments in order to conduct a Hanbury Brown-Twiss test. In essence, the Hanbury Brown-Twiss test will verify the particle nature of photons and confirm our understanding that photons are indivisible quanta of light. To conduct this test, we will be making some slight additions to our apparatus in order to measure the second-order correlation function. The value that we find for this function will provide a clear indication of quantum or classical behavior of the photons in our set-up. In a classical picture, the second-order correlation function is defined in terms of the intensity fluctuations of incident light at various detectors. In the quantum picture however, the second-order correlation function is defined in terms of coincidence events between detectors.

To conduct this experiment, we place a beam splitter along one path of down-converted photons leaving the other path undisturbed. By placing one detector along the transmitted path of the beamsplitter and another along the reflected path, we can see that as a photon enters the beamsplitter, it will either reflect or transmit, but **not** both. To be able to discuss the three detectors more easily, let the detector along the path with no beam splitter be called detector A, let the transmitted detector be called B, and the reflected detector be called C. Since photons are incident on the beam splitter at a very high rate, we must have an effective method of

determining when a photon is present at one detector or another. Furthermore, we want to be counting only the photons that are part of a down-converted pair as these exhibit the necessary statistical properties to conduct this Hanbury Brown-Twiss test. Because of this, we will be interested in the coincidence events between detectors A and B as well as between detectors A and C. By focusing our attention on the coincidence events, we can be sure that the data we are collecting is a result of down-converted photons interacting with the apparatus. Since we use the presence of a photon at detector A to infer the presence or absence of a photon at detectors B or C, we refer to the coincident photons at detector A as *heralding photons*. In theory, what we expect to see is that when a heralding photon is detected at A, another photon is detected at either the B or C detector, but there will never be a situation where a heralding photon is detected and then there is a photon found at both B **and** C at the same instant. In practice, this is more or less true, but there is still a very small chance that our detectors will register photons at all three detectors within the set coincidence window. It is important to note that these cases are not a result of a “down-converted triplet” but rather an experimental artifact arising from the fact that some ambient light could be getting into our detectors within the coincidence window. What this demonstrates is that as a heralding photon is detected, another photon enters the beam splitter and will transmit or reflect, but never will this photon split its energy and send a signal to both B and C. This interaction is what allows us to confirm that photons are truly quanta of electromagnetic radiation.

5.0.1 Theory

If we were to treat light as a classical wave in this situation, we would find that some of the wave intensity is transmitted and some reflected causing both detectors B and C to be triggered at the same time. However, this is not the case in our experimental set-up where we can consider our down-converted photons to be coming from a single photon source. The criteria necessary for a system to be a single photon source is as follows: the light emitted from the source must be generated via the excitation and emission from a *single* atom. This experimental set up that detects coincidences mimics this single photon source by generating single photon

states, or photons with the same energy. It is an experimental fact that single photon sources exhibit an intrinsically quantum phenomena known as anti-bunching. What this implies is that these photons obey sub-Poissonian statistics, or more specifically, the variance of the photon number distribution is strictly less than the mean of the distribution¹. Since photon counting is a statistical process, we will be interested in finding the various probabilities of registering a photon or coincidence event at certain detectors. These probabilities will be in terms of the measured quantities: the number of singles counts and coincidence counts. If we consider a set up like in Fig. 5.0.1, we may want to know the probability of registering a photon at detector B, detector C, and even the probability of a coincidence event between B and C even though we expect this to never occur. We can compute these the probabilities as

$$\mathcal{P}_B = \frac{N_{AB}}{N_A} \quad (5.0.1)$$

$$\mathcal{P}_C = \frac{N_{AC}}{N_A} \quad (5.0.2)$$

$$\mathcal{P}_{BC} = \frac{N_{ABC}}{N_A} \quad (5.0.3)$$

where N_A is the number of photons registered at detector A (singles counts), N_{AB} is the number of coincidence events between A and B, N_{AC} is the number of coincidence events between A and C, and N_{ABC} is the number of triple coincidences between A, B and C. Notice that all of these probabilities depend on the singles counts at the heralding detector A and the coincidences between detector A and one or both of the other two detectors. As well, notice that the probability of measuring a photon at detectors B and C involves triple coincidences N_{ABC} . Such triple coincidences are very uncommon, yet, as was stated above, given a certain coincidence window there is still a non-zero probability of registering such triple coincidences. Nonetheless, the unlikely nature of registering a triple coincidence should give some indication as to what we expect the value of \mathcal{P}_{BC} to be. With these probabilities at hand, the second-order

¹For a more detailed discussion of the second-order correlation function, photon counting statistics, bunching, anti-bunching, and single photon sources, see Fox, *Quantum Optics: An Introduction* (Oxford University Press, 2006), 108-122.

correlation function for this system can be written as²

$$g^{(2)}(0) = \frac{\mathcal{P}_{BC}}{\mathcal{P}_B \mathcal{P}_C} = \frac{N_{ABC} N_A}{N_{AB} N_{AC}}. \quad (5.0.4)$$

The uncertainty of the second-order correlation function can be estimated by considering the propagation of Poissonian statistical errors in the counts:

$$\Delta g^{(2)}(0) = g^{(2)}(0) \left(\frac{1}{\sqrt{N_{ABC}}} + \frac{1}{\sqrt{N_{AB}}} + \frac{1}{\sqrt{N_{AC}}} + \frac{1}{\sqrt{N_A}} \right). \quad (5.0.5)$$

And so, for an ideal single-photon source, meaning the photons exhibit anti-bunching, we expect $g^{(2)}(0) = 0$ mainly due to the fact that with regulated spacing between photons, we anticipate there to be very few triple coincidences compared to coincidence counts N_{AB} and N_{AC} . If we considered a classical electromagnetic wave exhibiting Poissonian statistics, we would expect there to always be a signal present at both B and C, thus the intensity correlations would give $g^{(2)}(0) \geq 1$.

The conclusion that $g^{(2)}(0) = 0$ for an ideal single-photon source comes from the fact that a detection in the heralding detector implies the presence of a photon in either the reflected or transmitted path of the beam splitter, but not both (hence the lack of triple coincidences). And so, the experimental goal is to measure the second-order correlation function as close to zero as possible, and then calculate the uncertainty in our measurements.

5.0.2 Experimental Procedure

Conducting a Hanbury-Brown Twiss test only requires a few additions to the SPDC set-up. The additional parts needed are as follows:

1. Beam Splitter (preferably a 50/50 BS cube)
2. 1 810nm line filter
3. Mounted fiber collimator and fiber optic cable

²This result is an experimentally accessible quantity presented by Galvez in his lab manual on this topic. For a more theoretical derivation of the classical or quantum form of the second-order correlation function, refer to Fox chapters 6.3 and 8.5.

Note that this list does not include the fact that one will also need an additional BNC cable and SPCM³.

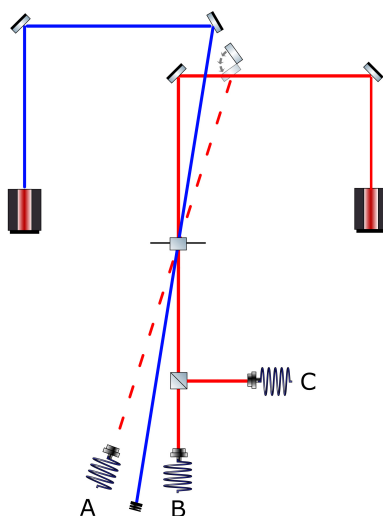


Figure 5.0.1. Hanbury-Brown Twiss experimental setup. Not included is the data acquisition system and further electronic elements used in data acquisition.

To set up these materials, use the alignment laser to first place the beam splitter (BS) somewhere along the beam path between the crystal and detector B. Make sure that the reflected beam is perpendicular to the transmitted beam. This point is not only crucial because we want the reflected and transmitted beam paths to be of similar lengths, but also because this BS can be used in the future to make a Mach-Zehnder Interferometer, the key apparatus for conducting a Quantum Eraser experiment. Although we are not making a Quantum Eraser here, it is still good to keep future possibilities in mind. Having placed the BS properly, the next step is to place the fiber collimator for detector C at the correct height off the table and the proper distance

³More details on data acquisition set-up can be found in Appendix A.

from the BS. The distance between the reflected and transmitted detectors to the BS should be roughly the same. This will make it so that both fiber collimators for B and C are collecting roughly the same number of down-converted photons. After placing this fiber collimator, use the alignment beam and fiber optic cable to maximize the amount of light being collimated. One should re-align the fiber collimator at detector B as well since the BS cube may have displaced the beam path. This can be done by eye or using an oscilloscope with a photodetector. Once detector C is placed, and both B and C are aligned, mount the 810nm line filters, turn off the alignment beam, and screw the fiber optic cables back into their respective SPCM's. In the end, the set up should resemble Fig 5.0.1.

5.0.3 Results and Discussion

By measuring singles counts per second on each detector, we can use the digitizer and CoMPASS software to store the timestamps of each detection in a table. We then use a MATLAB script to count coincidence events given the timestamp information from each detector and setting some coincidence window ΔT . With the data collected, the best result for the second-order correlation function was

$$g^{(2)}(0) = 0.04 \pm 0.012 \quad (5.0.6)$$

with a coincidence window $\Delta T = 7.59\text{ns}$. One aspect of this experiment that could have been better optimized was the efficiency at which down-converted pairs were produced. Because the GaN laser being used was not perfectly linearly polarized, it proved difficult to increase the number of coincidence events per second. In future experiments, having a linearly polarized pump laser would be optimal and would result in an easier time with the set up. Furthermore, obtaining a higher coincidence rate per second would allow for shorter data acquisition times. In this experiment, we took data for about 100 seconds in order to achieve accurate statistics.

In conclusion, this result implies a few things. Firstly, by measuring the second-order correlation function to be less than one, we have shown that the light source is sub-Poissonian in nature (exhibits anti-bunching). Having observed this fact, we can be sure that our down-converted photons have the characteristic qualities of a single-photon source. Furthermore, we

can infer from the result that a single photon incident on a beamsplitter acts purely as a particle and not as a wave. Thus we can conclude that a single photon is a quantum object that, when incident on a beam splitter, transmits or reflects, but in no way will split its energy such that some is transmitted and some reflected. In short, we have experimentally demonstrated that a single photon is an indivisible quanta of light. Moving on, we will see that we can use these single photon measurements along with the concept of entanglement to form a better understanding of quantum measurement as well as verify the non-local nature of quantum mechanics.

6

Bell's Theorem and Testing the Bell Inequality

6.1 Introduction to Bell's Theorem

Let's consider the following physical situation: two photons are created such that their quantum state is in a superposition of the horizontal and vertical basis states. The section on polarization entanglement from chapter 3 describes a physical process that will generate such a state. Having prepared two photons in this manner, we found that the state can be described as

$$|\Phi^+\rangle = \frac{1}{\sqrt{2}}(|H\rangle_1|H\rangle_2 + |V\rangle_1|V\rangle_2) = \frac{1}{\sqrt{2}} \begin{pmatrix} 1 \\ 0 \\ 0 \\ 1 \end{pmatrix}. \quad (6.1.1)$$

Then, we can imagine sending these two photons in distinct directions where both will interact with separate polarizers. After interacting with the polarizers, quantum mechanics tells us that the act of measuring the polarization of one of the photons causes the polarization state of **both** photons to immediately snap into one of the two possibilities (horizontal or vertical) at random. Furthermore, we can tell from the construction of $|\Phi^+\rangle$ that whatever polarization state we measure one photon to be in, the other photon, at some distance isolated from the measurement apparatus of the first photon, will be in the same polarization state! This phenomenon raises a very serious question regarding interpretation: was the polarization of the photon defined all along, or is the polarization only defined once a measurement has been made? A staunch

realist would say that all observable properties of these photons are completely defined upon their creation, and when we launch them into our measurement apparatus, they are simply in a statistical mixture of these definite properties. Unfortunately for the realists, and fortunately for the rest of us curious people, quantum mechanics implies something much different. Rather, what quantum mechanics can say about this entangled system is that the state of either photon is truly *undefined* prior to measurement.

The realist point of view, which judges the quality of a scientific theory by its predictive capability, was at the core of the EPR paper published in 1935 which argues for the incompleteness of quantum mechanics as a scientific theory. When this argument was presented to the physics community, many were convinced of the incompleteness of quantum mechanics, but a resolution to the so-called “EPR paradox” was not well understood until about three decades later. Then, in the early 1960s, to save us all from our collective ignorance, John Bell set out to find an answer to this discrepancy between quantum theory and the realist point of view. In the end, not only did he succeed in developing a mathematical framework capable of comparing quantum theory with the proposed “hidden-variable” theories, but he also derives a result that can be tested experimentally.

6.1.1 *The Bell Inequality*

In Bell's original paper, instead of thinking of polarization entangled photons, he considers a physical scenario first imagined by David Bohm as a simplification to the original EPR thought experiment. This scenario is as follows: Imagine a pion at rest that decays into an electron and positron pair which travel in opposite directions to each other. Then, these two particles travel towards independent detectors that measure the spin of the incident particle along some particular measurement axis.

Let the measurement axes for the electron and positron detectors be denoted \vec{a} and \vec{b} respectively. In the case where the spin measurements for both particles are made along the same axis (i.e. $\vec{a} = \vec{b}$), we will measure one particle to have spin up and the other spin down with absolute certainty. Note that a spin up measurement takes on the value +1, and a spin down measure-

ment takes the value -1 . For this case, the average (or expectation value) of the **products** of spin measurements is

$$E(\vec{a}, \vec{b}) = E(\vec{a}, \vec{a}) = -1. \quad (6.1.2)$$

In a similar fashion, if the detectors axes are anti-parallel ($\vec{a} = -\vec{b}$) then

$$E(\vec{a}, \vec{b}) = E(\vec{a}, -\vec{a}) = 1. \quad (6.1.3)$$

And for arbitrary orientations of detector axes, we have that

$$E(\vec{a}, \vec{b}) = -\vec{a} \cdot \vec{b}. \quad (6.1.4)$$

These are the predictions of quantum mechanics, and from now on we can refer to Eq. 6.1.4 as the quantum mechanical expectation value. What Bell realized (and as we will show) is that this prediction is incompatible with *any* local hidden-variable theory.

Let us now make a claim (Bell's hypothesis): If the two measurements are made at distinct locations, the measurement outcome of one particle does not influence the result obtained by measuring the other particle. If we suppose this claim to be true, then it must be the case that both the electron and positron had definite spin prior to measurement (contrary to what quantum mechanics tells us). Taking this to be true for now, there must be some more complete description of the state of the two particles according to the realist point of view, and this description must be characterized by some unknown (or "hidden") variable that we will call λ . Then, there must exist some functions that will completely pre-determine the measurement outcomes for the spin of the electron and positron respectively. These functions will be dependent on the detector orientations and the unknown variable λ . For the electron, we denote this function $A(\vec{a}, \lambda)$, and for the positron $B(\vec{b}, \lambda)$. It follows from what we know about the possible outcomes of the spin measurements that

$$A(\vec{a}, \lambda) = \pm 1 \text{ and } B(\vec{b}, \lambda) = \pm 1. \quad (6.1.5)$$

As well, when the detector axis are equal ($\vec{a} = \vec{b}$), we have that

$$A(\vec{a}, \lambda) = -B(\vec{a}, \lambda), \quad (6.1.6)$$

indicating perfect anti-correlation of the measurement outcomes. Then, in this “more complete” formulation that includes hidden variable λ , the expectation value of the product of measurement outcomes is

$$E(\vec{a}, \vec{b}) = \int \rho(\lambda) A(\vec{a}, \lambda) B(\vec{b}, \lambda) d\lambda \quad (6.1.7)$$

where $\rho(\lambda)$ is a probability density function for the hidden variable. Note that we know nothing specific about λ and so we know nothing specific about $\rho(\lambda)$ either, but yet we are “integrating out” all of the unknown information and so we will be perfectly capable of working with $\rho(\lambda)$ in this context. By substitution, notice

$$E(\vec{a}, \vec{b}) = - \int \rho(\lambda) A(\vec{a}, \lambda) A(\vec{b}, \lambda) d\lambda. \quad (6.1.8)$$

Now consider some third possible measurement axis \vec{c} . Note that no detectors or extra measurement devices are being added, we are simply considering a new distinct measurement axis which we could measure the spin along if we chose to. By doing so, we can learn something about how the expectation values of the product of measurement outcomes differ from each other depending on the measurement axes considered. Then, by taking the difference of $E(\vec{a}, \vec{b})$ and $E(\vec{a}, \vec{c})$, notice

$$E(\vec{a}, \vec{b}) - E(\vec{a}, \vec{c}) = - \int \rho(\lambda) [A(\vec{a}, \lambda) A(\vec{b}, \lambda) - A(\vec{a}, \lambda) A(\vec{c}, \lambda)] d\lambda. \quad (6.1.9)$$

Notice that since $[A(\vec{b}, \lambda)]^2 = 1$, we can rewrite the previous equation in the form

$$E(\vec{a}, \vec{b}) - E(\vec{a}, \vec{c}) = - \int \rho(\lambda) [1 - A(\vec{b}, \lambda) A(\vec{c}, \lambda)] A(\vec{a}, \lambda) A(\vec{b}, \lambda) d\lambda. \quad (6.1.10)$$

Then, given what we know about the possible values of $A(\vec{a}, \lambda)$, it follows that $|A(\vec{a}, \lambda) A(\vec{b}, \lambda)| = 1$. Also, since $\rho(\lambda)$ is always positive and $A(\vec{b}, \lambda) A(\vec{c}, \lambda) = \pm 1$, it follows that $\rho(\lambda) [1 - A(\vec{b}, \lambda) A(\vec{c}, \lambda)] \geq 0$. Using these two facts, we can conclude that

$$|E(\vec{a}, \vec{b}) - E(\vec{a}, \vec{c})| \leq \int \rho(\lambda) [1 - A(\vec{b}, \lambda) A(\vec{c}, \lambda)] d\lambda. \quad (6.1.11)$$

One can use the triangle inequality to see this more clearly. Then, by simplification, we conclude

$$\boxed{|E(\vec{a}, \vec{b}) - E(\vec{a}, \vec{c})| \leq 1 + E(\vec{b}, \vec{c})}. \quad (6.1.12)$$

This is Bell's inequality in the form that John Bell first published in 1964.

So, by making very few assumptions (one of them certainly being local realism), Bell was able to derive an inequality that should be true for *any* local hidden variable theory since we made no particular assumptions regarding λ . Furthermore, Bell provided an epsilon-delta proof demonstrating the incompatibility of the hidden-variable expectation value with the quantum mechanical expectation value. What this shows is that **no** hidden variable theory can be constructed that will provide the same predictions as the quantum mechanical expectation value (which does make accurate statistical predictions). By deriving this inequality in the context of a physically realizable scenario, Bell reignited some hope that perhaps an experiment could be constructed to test this inequality thus confirming the completeness of quantum mechanics!

What Bell's proof tells us about quantum mechanics is that (1) it is truly a complete theory since no more complete theory can exist and (2) it is fundamentally non-local since we contradicted our hypothesis which rested firmly on the assumption of locality. Note that by non-local, we do not mean that there exist super-luminal effects between the detectors. This is because no information is passed between measurement devices during the measurement process. This would be known as a *causal influence*. That is to say, nothing that happens at one detector can cause anything to happen at the other one. Now, surely the measurement outcome of one detector *influences* the outcome of the other detector, but this is certainly different than if the detection sparked some instantaneous switch that then communicated the proper outcome to the other detector. Surely this is a subtle and nuanced discussion that deserves a more rigorous discussion, but in principle, it is important to note that we are not violating relativistic causality (the idea that no information can travel faster than the speed of light) by claiming the presence of non-local effects.¹

In addition to the inequality in the form that Bell originally derived, there is another inequality, which turns out to be equivalent, that we can derive from Bell's hidden variable assumptions and is more easily applied to experimental data. In particular, this other inequality takes into

¹For a deeper conceptual discussion on this topic and further topics such as decoherence, see Griffiths & Schroeter, *Introduction to Quantum Mechanics* (Cambridge University Press, 2018), 446-453 and 461-463.

account the imperfect nature of real life detectors, and is very useful when doing experiments using polarization entangled photons. We call this inequality the Clauser-Horne-Shimony-Holt (CHSH) inequality after the four people who are credited for its derivation. The way in which the CHSH inequality accounts for imperfect detectors is by allowing for the possibility that a measurement yields no outcome since there is always the possibility that a detector fails to register something even when a signal is present. A measurement that fails to register the presence of a signal is given the value of 0.

Starting with hidden-variable expectation value

$$E(\vec{a}, \vec{b}) = \int \rho(\lambda) A(\vec{a}, \lambda) B(\vec{b}, \lambda) d\lambda, \quad (6.1.13)$$

we can introduce two new measurement axes \vec{a}' for one detector, and \vec{b}' such that

$$E(\vec{a}, \vec{b}) - E(\vec{a}, \vec{b}') = \int \rho(\lambda) [A(\vec{a}, \lambda) B(\vec{b}, \lambda) - A(\vec{a}, \lambda) B(\vec{b}', \lambda)] d\lambda. \quad (6.1.14)$$

Then, we may re-write this equality (for reasons that are not obvious now but will become clear soon) as

$$\begin{aligned} E(\vec{a}, \vec{b}) - E(\vec{a}, \vec{b}') &= \int \rho(\lambda) [A(\vec{a}, \lambda) B(\vec{b}, \lambda) - A(\vec{a}, \lambda) B(\vec{b}', \lambda)] d\lambda \\ &= \int \rho(\lambda) [A(\vec{a}, \lambda) B(\vec{b}, \lambda) - A(\vec{a}, \lambda) B(\vec{b}', \lambda) \\ &\quad \pm A(\vec{a}, \lambda) B(\vec{b}, \lambda) A(\vec{a}', \lambda) B(\vec{b}', \lambda) \mp A(\vec{a}, \lambda) B(\vec{b}, \lambda) A(\vec{a}', \lambda) B(\vec{b}', \lambda)] d\lambda \\ &= \int \rho(\lambda) A(\vec{a}, \lambda) B(\vec{b}, \lambda) [1 \pm A(\vec{a}', \lambda) B(\vec{b}', \lambda)] d\lambda \\ &\quad - \int \rho(\lambda) A(\vec{a}, \lambda) B(\vec{b}', \lambda) [1 \mp A(\vec{a}', \lambda) B(\vec{b}, \lambda)] d\lambda. \end{aligned} \quad (6.1.15)$$

Then, by taking the absolute value and using the triangle inequality ($|\vec{x}| - |\vec{y}| \leq |\vec{x} + \vec{y}| \leq |\vec{x}| + |\vec{y}|$) we can see that

$$\begin{aligned} |E(\vec{a}, \vec{b}) - E(\vec{a}, \vec{b}')| &\leq \left| \int \rho(\lambda) A(\vec{a}, \lambda) B(\vec{b}, \lambda) [1 \pm A(\vec{a}', \lambda) B(\vec{b}', \lambda)] d\lambda \right| \\ &\quad + \left| \int \rho(\lambda) A(\vec{a}, \lambda) B(\vec{b}', \lambda) [1 \pm A(\vec{a}', \lambda) B(\vec{b}, \lambda)] d\lambda \right|. \end{aligned} \quad (6.1.16)$$

Then, since the each component of the integrands are non-negative, we can use what we know about the absolute values of products to write

$$|E(\vec{a}, \vec{b}) - E(\vec{a}, \vec{b}')| \leq \int |A(\vec{a}, \lambda)B(\vec{b}, \lambda)| |1 \pm -A(\vec{a}', \lambda)B(\vec{b}', \lambda)| \rho(\lambda) d\lambda \\ + \int |A(\vec{a}, \lambda)B(\vec{b}', \lambda)| |1 \pm A(\vec{a}', \lambda)B(\vec{b}, \lambda)| \rho(\lambda) d\lambda. \quad (6.1.17)$$

Since we know $|A| \leq 1$ and $|B| \leq 1$ for any measurement axis, we may remove those pieces from the inequality to simplify such that

$$|E(\vec{a}, \vec{b}) - E(\vec{a}, \vec{b}')| \leq \int [1 \pm -A(\vec{a}', \lambda)B(\vec{b}', \lambda)] \rho(\lambda) d\lambda + \int [1 \pm A(\vec{a}', \lambda)B(\vec{b}, \lambda)] \rho(\lambda) d\lambda \quad (6.1.18)$$

$$= 2 \pm \left[\int A(\vec{a}', \lambda)B(\vec{b}', \lambda) \rho(\lambda) d\lambda + \int A(\vec{a}', \lambda)B(\vec{b}, \lambda) \rho(\lambda) d\lambda \right] \quad (6.1.19)$$

$$= 2 \pm [E(\vec{a}', \vec{b}') + E(\vec{a}', \vec{b})]. \quad (6.1.20)$$

Note that the 2 comes from the fact that $\int \rho(\lambda) d\lambda = 1$, and we did this twice.

So, in a cleaner form we may write

$$|E(\vec{a}, \vec{b}) - E(\vec{a}, \vec{b}')| \leq 2 \pm [E(\vec{a}', \vec{b}') + E(\vec{a}', \vec{b})], \quad (6.1.21)$$

and since $2 + [E(\vec{a}', \vec{b}') + E(\vec{a}', \vec{b})] > 2 - [E(\vec{a}', \vec{b}') + E(\vec{a}', \vec{b})]$ we can write even more simply

$$|E(\vec{a}, \vec{b}) - E(\vec{a}, \vec{b}')| \leq 2 - |E(\vec{a}', \vec{b}') + E(\vec{a}', \vec{b})|. \quad (6.1.22)$$

Hence

$$2 \geq |E(\vec{a}, \vec{b}) - E(\vec{a}, \vec{b}')| + |E(\vec{a}', \vec{b}') + E(\vec{a}', \vec{b})| \geq |E(\vec{a}, \vec{b}) - E(\vec{a}, \vec{b}') + E(\vec{a}', \vec{b}') + E(\vec{a}', \vec{b})| \quad (6.1.23)$$

where the last inequality follows from applying the triangle inequality again.

To make this look a bit nicer, let $S = E(\vec{a}, \vec{b}) - E(\vec{a}, \vec{b}') + E(\vec{a}', \vec{b}') + E(\vec{a}', \vec{b})$. Then, the final inequality, which places constraints on the statistics of these joint detections, is

$$\boxed{|S| \leq 2}. \quad (6.1.24)$$

It is this inequality that we will try to violate in order to confirm the completeness of quantum mechanics. As well, one can see that this is actually just a special case of the original Bell inequality.

To see this, let $\vec{a}' = \vec{b}'$ and assume that $E(\vec{b}', \vec{b}') = -1$. Then, we have

$$|E(\vec{a}, \vec{b}) - E(\vec{a}, \vec{b}')| + |E(\vec{a}', \vec{b}') + E(\vec{a}', \vec{b})| = |E(\vec{a}, \vec{b}) - E(\vec{a}, \vec{b}')| + |(-1) + E(\vec{a}', \vec{b})| \leq 2. \quad (6.1.25)$$

By subtracting $|(-1) + E(\vec{a}', \vec{b})|$ from both sides of the inequality

$$|E(\vec{a}, \vec{b}) - E(\vec{a}, \vec{b}')| \leq 2 - |(-1) + E(\vec{a}', \vec{b})|, \quad (6.1.26)$$

and since $|(-1) + E(\vec{a}', \vec{b})| \leq |-1| + |E(\vec{a}', \vec{b})|$ by the triangle inequality, we conclude that

$$|E(\vec{a}, \vec{b}) - E(\vec{a}, \vec{b}')| \leq 1 + E(\vec{a}', \vec{b}) \quad (6.1.27)$$

which is of the same form that Bell first derived as we saw above.

So, having derived Bell's inequality in two forms, let us take a moment to restate the argument. Given an experimental apparatus that produces pairs of physical systems, we can make many measurements over a period of time by simply running the experiment many times and collecting the results from each. For any iteration of the experiment, we are only capable of making a measurement on one of the four possible joint detection outcomes (two detectors each with two possible detection axes). Thus by repeating these four possible joint measurements repeatedly, we are capable of sampling the statistics of each result giving us an expectation value for the four joint detections. So, if the universe is governed by some sort of hidden-variable theory, our experimental test will confirm that the statistical inequality we derived is consistent with reality. However, when conducting an experiment with real data, it has been found that for particular measurement axes, the experimental results violate the statistical inequality we derived, proving that quantum mechanics is incompatible with any local hidden-variable theory and furthermore, is a complete theory. Moving forward, we discuss the assumptions of the EPR thought experiment that inspired Bell to embark on his journey towards understanding some very fundamental aspects of quantum mechanics. In particular, we investigate how Bell's results influence our notion of what it means to make quantum mechanical measurements as well as our ability to interpret the predictions of quantum theory.

6.1.2 Thought Experiment Version of Bell's Inequality

When EPR first proposed their thought experiment, they were guided by a few underlying principles. Firstly, they claim that when given two correlated particles, some characteristics of one may be precisely determined without direct measurement on that particle. This is done simply by only measuring the characteristic of one particle, and due to their correlated nature, we may infer some information regarding the physical characteristic of the other particle. At the onset, this claim is nothing surprising or against what we already know to be true regarding physical reality. Subsequently, EPR claim that this physical situation must imply that the characteristic of one particle, which was inferred by directly measuring the correlated particle (and *only* the other particle), must be some type of “element of reality” that exists regardless of our measurement process. This assumption is based upon the philosophical concept called *Scientific Realism*, and is defined in the following manner: Scientific Realism is the philosophical stance that measurable characteristics of a physical system exist and are well defined independent of any observers or external influence. Furthermore, this implies that the goal of a scientific theory is to produce an ideal model of reality that can accurately and precisely predict measurement outcomes of physical characteristics.

The second assumption made by EPR is one based upon the philosophy of *determinism*, or the idea that the physical “elements” or characteristics of a system evolve through time and space in a predictable manner such that information regarding the current state of a system can be used to determine the future state of that system. As we well know, quantum mechanics does *not* predict definite measurement outcomes of physical characteristics. Rather, quantum mechanics can only make statistical predictions regarding measurement outcomes. EPR never took issue with the ability of quantum theory to make accurate statistical predictions, rather they were of the philosophical belief that a scientific theory is only complete when it can fully describe and predict every measurable characteristic of a physical system (an ideal theory). Since quantum mechanics very clearly does not meet these criteria, EPR claimed that it must be incomplete.

So, what consequences do these two philosophical assumptions have on our understanding of physical reality? Well, there are two big ones that we will certainly want to keep in mind moving forward. Firstly, the EPR assumptions imply that all physical properties of a system have definite value even if not measured. Secondly, these assumptions imply that the measurement of a particle at one location does not effect the result of a measurement made at a distinctly separate location. This concept is known as *locality*. On the subject of locality, Einstein was particularly curious about the issue of causality in quantum mechanics, and was concerned that by allowing for the possibility of non-local effects, the concept of relativistic causality would be contradicted. Thus EPR were unable to accept the idea that perhaps certain characteristics of a physical system are dependent on particular non-local effects. This fact is at the heart of the paradox that we find ourselves in when trying to make sense of experimental results that violate Bell's inequality. It is the fact that the values of certain physical properties of a system **do** depend on non-local effects that makes the EPR argument non-representative of our physical reality. This idea regarding non-local effects goes against lots of the "common sense" that we all live by in our daily lives, yet it is truly at the heart of what makes Bell's theorem such an illuminating result.

Having laid out the basic underlying assumptions of the EPR argument and their important implications, let's conduct a thought experiment to see how these assumptions fail to capture the reality predicted by quantum mechanics. From now on, we will refer to results related to the EPR assumptions as the "common sense" results. For our thought experiment, we will consider two polarized entangled photons. In this case, as it will be useful in our analysis, note that for a photon polarized along angle ϕ_2 , the component of the amplitude that lies along the polarizer axis ϕ_1 is given by $\cos(\phi_2 - \phi_1)$. Thus the probability that a photon polarized along some direction ϕ_2 transmits through a polarizer ϕ_1 is this transmission amplitude squared given by $\cos^2(\phi_2 - \phi_1)$. We will compare this quantum mechanical result with the "common sense" way of looking at things. Now we are well prepared to begin our thought experiment.

Suppose we have set up our experimental apparatus such that we generate perfectly correlated photon pairs (described by $|\Phi^+\rangle$ from chapter 3) and they get sent to two measurement devices

at separate locations that have polarizing filters in front of them. Let the angle of one polarizer be denoted θ_1 and the other θ_2 . When the polarizers are set along the same direction $\theta_1 = \theta_2$, and the photon pairs have the same polarization also equal to the polarizer axes, our equation for the probability of transmission indicates that the 100% of the time we expect both photons to pass through their respective polarizers and interact with the measurement devices. Thus if we were to take a sequence of measurements with these polarization settings, each individual measurement would indicate that the two photons are always measured to be in the same state. In a similar way, if the polarizers are oriented perpendicularly to each other, our equation tells us that 0% of the time should we expect to both photons to pass through the polarizer. Given these two extreme cases, it seems reasonable (common-sensical even) to think that for measurements made at angles between 0° and 90° , there would be a continuous range of probabilities (or correlation) ranging from 0% to 100%. Let's see if this is the case.

Take some angle α where $0^\circ \leq \alpha \leq 90^\circ$, and suppose that the probability that both photons go through their respective polarizers is 75% (meaning 25% of the time one photon passes and the other does not). We call the events where both photons transmit *coincidences*, and so when the probability of both going through is 75%, we can say that the average coincidence rate is that value. So, if we let $\theta_1 = 0$ and $\theta_2 = \alpha$, we say that the average coincidence rate is 75%. The same should be true for when $\theta_1 = -\alpha$ and $\theta_2 = 0$. Because in each of these cases the average mismatch (non-coincidence) rate is 25%, we may expect that for the settings $\theta_1 = -\alpha$ and $\theta_2 = \alpha$ that the average mismatch rate should be 50% (the sum of the average mismatch rate for the two individual cases). This is the “common sense” prediction. Furthermore, this kind of constraint on what we *expect* is an example of a Bell inequality.

Now let us see how this “common sense” prediction stands up against the quantum mechanical prediction (and experimental results). We claimed, starting from very basic assumptions (and those of EPR), that at the mismatch rate should be no greater than 50%. However, if we look back to our quantum prediction for the coincidence rate, we find that a mismatch rate of 25% occurs for $\alpha = \theta_2 - \theta_1 = 30^\circ$, meaning the coincidence rate is $\cos^2(30^\circ) = 0.75$. Then, if we use

our “common sense” result, we should expect that the mismatch rate for when $\alpha = \theta_2 - \theta_1 = 60^\circ$ should be no greater than 50%, yet notice $\cos^2(60^\circ) = 0.25$. This implies that the mismatch rate for this case is 75%, which is certainly greater than the 50% predicted by our “common sense” logic. This is an example of violating Bell’s inequality, and to try and understand where the “common sense” result goes astray, we must reexamine the logical deduction that brought us to such conclusions in the first place.

For the true skeptic, one may think that in reality there may not even exist an angle α where the mismatch rate is 25% like initially claimed, but this is not the case as experimental observation has confirmed. In actuality, the trouble in the initial argument lies in the last step where we assume certain things about going from the $\theta_1 = -\alpha$ and $\theta_2 = 0$ case to the $\theta_1 = -\alpha$ and $\theta_2 = \alpha$ case. When changing between these cases, one must actually rotate the second polarizer from initial position 0 to angle α . When this occurs, we had assumed implicitly that this process would not affect the sequence of results collected by the other (untouched) filter. That is to say, we assumed that the sequence of results collected at one filter will be the same regardless of the position of the other filter. In our “common sense” logic, this followed from the assumption of locality. This assumption is what leads one astray, and a more accurate picture of the reality is only restored when we allow for the possibility that rotating the filter at one location actually **does** affect the sequence of results acquired at the other detector. By allowing for this possibility, we are accepting that there are non-local effects at play, yet without contradicting relativistic causality. In closing, what this explanatory way of viewing Bell’s inequality reveals to us is that we cannot make accurate predictions on these quantum systems unless we consider the possibility for non-local effects. In the next section, there will be an experimental presentation of this same type of argument, and with these experimental results, we hope to confirm by direct observation that the predictions of quantum mechanics accurately reflect physical reality.²

²This section was heavily influenced by Guy Blaylock’s paper entitled *The EPR paradox, Bell’s inequality, and the question of locality*.

6.2 Bell Test Experimental Procedure

In the chapter on entanglement, we discussed quite a bit about a physical process that generates down-converted photon pairs that are polarization entangled. Here we go through the experimental procedure to generate and confirm the detection of polarization entangled photon pairs. With the capability to generate and detect polarization entangled photons, we will be well prepared to do a physical test of Bell's inequality, often called a Bell Test. The parts needed for this test are as follows:

1. 1 BBO crystal pair (X)
2. 1 405nm, zero order Half-wave plate (V)
3. 1 Compensating quartz crystal (A-cut, 6-8mm thick in a rotation mount) (U)
4. 2 810nm, zero order Half-wave plates (H)
5. 2 Glan-Thompson polarizers (P)

Note that the BBO crystal pair could have been used for the previous experiments as well although not necessary. For the Bell Test however, it is essential to have this crystal pair in order to generate a quantum state in which the two photons are both in a superposition of the horizontal-vertical polarization basis states.

The first step in this procedure is to simply mount all of the new optical elements in their proper rotating mounts and place them on the optical table in the correct fashion according to Fig 6.2.1. As well, if one has just completed a Hanbury Brown-Twiss test prior to this, they must take away detector C and remove the beam splitter cube from one of the beam paths. By disassembling these old pieces and adding some of these new elements, one could potentially misalign the beam into the fiber collimators. To fix this, place all new optical elements and then use the red alignment beam to re-align the fiber collimators. Return to the section on SPDC for an explanation of how to align the fiber collimators. Having gone through these preliminary steps, the procedure for producing and detecting polarization entangled photons is as follows:

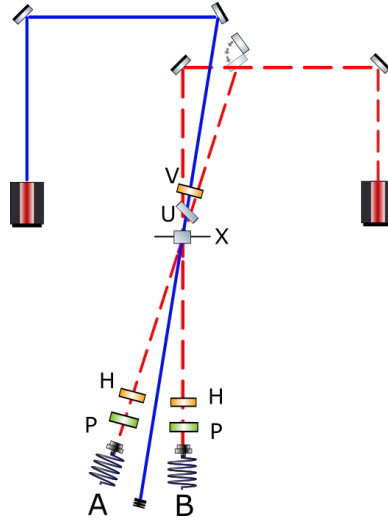


Figure 6.2.1. Polarization Entanglement and Bell Test set-up. Polarizers (P) choose which polarization state to detect, half-wave plates (H) are able to change the polarization of the incoming photons before they enter polarizer (P). The compensating quartz crystal (U) before the down-converting BBO crystal (X) allows for proper state production so that the photon pairs are in a superposition of polarization states, and half wave plate (V) allows for the changing of the pump beam polarization. Notice that the quartz crystal (U) is tilted to indicate that to maximize coincidence counts, one will need to tilt the crystal about the vertical axis to find the proper amount of compensation to produce the correct polarization.

1. Set the polarizers (P) to horizontal transmission. Then set half-wave plates (H) to 45° (this will change the incoming photons polarization by 90°). Then set half-wave plate (V) to 0° (this will do nothing to the pump polarization). Having set these elements in this way, this apparatus has been set to produce and detect down-converted photons that are vertically polarized.
2. Turn on the data acquisition system and set it up so that you can see the coincidences on each detector in live time (this is assuming that your detectors were already collecting an appropriate amount of singles counts as well). Then, begin to rotate the BBO crystal (X) in its mount in order to maximize coincidence counts. With our BBO crystal, we found this to be at 180° in the rotation mount. One indication that pairs are being detected is if they have the same polarization. Thus if you set one half-wave plate (H) to detect horizontally polarized photons and the other vertical, you should detect no coincidences if the pairs have the same polarization.

3. Now we can set the half-wave plate (V) to about 22.5° to make the pump beam diagonally polarized. Then, if they are not set like this already, set the half-wave plates (H) such that the photons entering the polarizers (P) are horizontally polarized (back to 0° assuming the polarizers (P) are still set to horizontal transmission). One should be able to get the same number of coincidences when setting the half-wave plates to detect horizontally polarized pairs and vertically polarized pairs.

4. All that is left is to use the quartz crystal to compensate one component of the pump beam by the proper amount so that we are producing entangled states. We do this by setting one half-wave plate to detect diagonally polarized light and the other to detect anti-diagonally polarized light. Assuming the polarizers (P) are still set to horizontal transmission, one can set one of the half-wave plates to 22.5° and the other to 67.5° to achieve this result. Due to the time delay of the creation of down-converted pairs, there is a phase shift in one component of the state vector

$$|\psi'\rangle = \frac{1}{\sqrt{2}}(|H\rangle_1|H\rangle_2 + |V\rangle_1|V\rangle_2 e^{i\delta}). \quad (6.2.1)$$

We expect that when $\delta = 0$ there will be no coincidences since one detector is set to detect D polarization and the other A polarization. Yet, when $\delta = \pi$ there will be coincidences, So, in order to get $\delta = 0$ as we would like since we need to have the down-converted pairs be indistinguishable, we can start adjusting the tilt of the quartz crystal relative to the vertical axis. This quartz crystal introduces another phase shift to one component of the beam, and the amount of phase shifting depends on the effective thickness of the quartz. Thus we rotate the quartz about the vertical axis until we reach as few coincidences as possible (indicating that we have eliminated the phase factor). Note here that the axes for the two indices of refraction of the quartz crystal should be aligned with the polarization components of the pump photon. It was found in our test that tilting the quartz crystal about 45° relative to the vertical axis gave the least number of coincidences per second.

Once this is complete, we have successfully made $\delta = 0$, and so we successfully prepared our entangled state.

6.2.1 Results and Discussion

When collecting data for the Bell Test, we made 16 measurements for which the angle between polarizer axes were different. One can leave the polarizers (P) untouched set to horizontal transmission and use the half-wave plates to make all measurements, but we opted to remove the half-wave plates and just rotate the polarizers as these rotation mounts were more precise. Then, using the formula for S in the CHSH inequality, we calculated from the data that

$$S = 1.15 \pm 0.025, \tag{6.2.2}$$

which, unfortunately, does not violate the inequality as we had hoped. Even more unfortunate, we did not have enough time to try and remedy our possible errors and collect new data.

There were a couple of factors that could have made for this undesirable result. Mainly, we had coincidence counts per second on the order of 10 to 20 per second, and due to so few coincidences per second, we needed to take data for about 500s per measurement in order to get somewhat accurate statistics. Because we had so few coincidences per second, there is the possibility that we did not accurately eliminate the phase factor δ which is essential in order to generate the polarization entangled state desired. The effect of tilting the quartz crystal on the phase factor would have been much more noticeable if we had more coincidences per second. It is very possible that the lack of coincidences per second was due to a polarizer being used on the pump beam in order to put the pump photons in the correct polarization state needed to generate down-converted pairs with the appropriate polarization. In previous experiments, we did not need to worry about the pump photon polarization, and thus this was not an issue in those tests. In future experiments, using a laser that is already perfectly linearly polarized would certainly help this issue.

A	B	$N(\theta_1, \theta_2)$
45	22.5	281
45	112.5	465
135	22.5	281
135	112.5	2561
45	67.5	1544
45	157.5	3127
135	67.5	978
135	157.5	674
0	22.5	354
0	112.5	2136
90	22.5	280
90	112.5	3715
0	67.5	448
0	157.5	1039
90	67.5	2086
90	157.5	321

Table 6.2.1. Displayed are the polarizer settings A and B used to violate the Bell inequality where $N(\theta_1, \theta_2)$ is the number of coincidences counted over the entire 500s data collection interval.

6.3 Von Neumann Model of Measurement and Decoherence

In all of the chapters of this text, we have been referring to the idea of making measurements on a system without actually discussing the concept or theory behind making measurements. Measurement is certainly a crucial feature in our ability to connect scientific theories with observed physical reality, but we often talk about measurement in abstract terms without actually giving it any formal attention. In classical physics, there is usually good reason to not be so concerned with a formal discussion of measurement. For example, suppose we have an object \mathfrak{G} that we observe or measure (e.g. a planet, electric current, or atomic transition) using a measurement device \mathfrak{U} (e.g. a telescope, ammeter, or photo-detector). Then, we can imagine that making a measurement involves a physical interaction $I_1 = I_{\mathfrak{G} \leftrightarrow \mathfrak{U}}$ between the object being measured \mathfrak{G} and the measurement device \mathfrak{U} . Not only does this measurement involve the interaction between the object and the measurement device, but also an interaction I_2 between the measurement device \mathfrak{U} and an observer \mathfrak{D} (a human's consciousness perceiving and interpreting the data collected by the measurement device). In principle, this fact that making a measurement also implies an interaction between the device and a human observer means that ultimately the relationship

between physical reality and our ability to measure it involves human consciousness to some degree. This poses an issue if we are to believe that scientific truth can exist outside of the presence of human consciousness. How can we say anything objective about the physical entities comprising our universe if making measurements intrinsically involves interactions with human consciousness? Here is one way of making these issues negligible: Consider the fact that an interaction $I_{\mathfrak{G} \leftrightarrow \mathfrak{U}}$ can be broken down into an action $I_{\mathfrak{G} \rightarrow \mathfrak{U}}$ where the object \mathfrak{G} acts on device \mathfrak{U} and another action $I_{\mathfrak{U} \rightarrow \mathfrak{G}}$ where the device \mathfrak{U} acts on the object being measured \mathfrak{G} . In a classical setting where we are observing macroscopic phenomena in general, we can consider the order of magnitude of $I_{\mathfrak{U} \rightarrow \mathfrak{G}}$ to be much less than that of $I_{\mathfrak{G} \rightarrow \mathfrak{U}}$. Because of this fact, we can neglect the effect that $I_{\mathfrak{U} \rightarrow \mathfrak{G}}$ has on the results of a measurement, and furthermore this allows us to ignore the impact that an interaction between device \mathfrak{U} and observer \mathfrak{D} may have on the main interaction of interest $I_{\mathfrak{G} \leftrightarrow \mathfrak{U}}$. Thus we have found a way of ignoring the role that human consciousness plays in making classical measurements since we have devised a stratagem that does not allow for any observer to effect the object being probed. However, things are not so cut and dry when considering making measurements on a quantum system.

The main issue of imposing this scheme on quantum systems is that we cannot ignore or neglect the interactions between the object \mathfrak{G} and measurement device \mathfrak{U} . For instance, we can consider quantum systems that operate at the Planck scale, and furthermore a measurement device sensitive to such scales may operate at a similar order of magnitude. In this case, the interactions $I_{\mathfrak{U} \rightarrow \mathfrak{G}}$ and $I_{\mathfrak{G} \rightarrow \mathfrak{U}}$ may have the same order of magnitude. Thus our classical stratagem is thrown out the window and is useless when trying to understand the meaning of making measurements on quantum systems.³

One very impactful theory of measurement in the quantum regime was put forth by physicist John von Neumann in his book on the mathematical foundations of quantum mechanics in 1932. This von Neumann model of measurement has proven to be an important contribution to the study of quantum interpretation as it opened the door to a new way of framing the

³This discussion was heavily influenced by Max Jammer's writing. See Jammer, *The Philosophy of Quantum Mechanics* (John Wiley & Sons, Inc, 1974), 471-482.

issue of quantum measurement. Here we will give a very brief account of this model. Firstly, von Neumann chose to construct a model of measurement in which all things had a quantum mechanical nature. Thus we can treat every object as having a wave function attributed to it. Suppose there is a quantum system Q that we would like to measure using another quantum system M , the measuring device. Then, somewhat similarly to the classical case, a measurement is an interaction between quantum systems Q and M . When a measurement of Q is made, there is an associated observable quantity A that is to be determined by M . There are many ways in which a measurement device may register the observable A , but for simplicity von Neumann allowed M to have only one degree of freedom such as the position X of a pointer on a meter or ruler.

We can assume that initially, the pointer is at the zero position, and since we have attributed a quantum character to the measurement device M , we can say that its initial wave function $\phi(x)$ is a narrow peak centered at the zero position ($x = 0$). Then, as previously stated, a measurement is an interaction between Q and M , and this interaction is described by the Hamiltonian $H_{\text{int}} = -g(t)AP$. First, note that the binary operation between A and P is operator multiplication (matrix multiplication), and note that A is the observable quantity being measured and P is the momentum operator associated with the pointer on the measurement device. Then, at the time of the interaction between Q and M , the scalar function $g(t)$ becomes large and positive for a short time interval Δt immediately after the interaction begins ($t = 0$), and then goes to zero right after the short interval ends. By virtue of this behavior, the interaction Hamiltonian is greatest during this short time interval and effectively zero otherwise. As well, this largeness of $g(t)$ within the short time interval Δt can be made as large as desired according to the particular interaction being considered. Because of this, we can consider the action of the physical process

$$\int_0^{\Delta t} H(t) dt \tag{6.3.1}$$

and by letting $\lambda = \int_0^{\Delta t} g(t) dt$, which dominates the interaction Hamiltonian during the interaction interval, we can write the time evolution operator for the composite system $U(0, \Delta t) =$

$e^{-\frac{i}{\hbar} \int_0^{\Delta t} H(t) dt}$, in the form

$$U(0, \Delta t) = e^{-\frac{i}{\hbar} \lambda A P}. \quad (6.3.2)$$

Then, further expressions for the time evolution operator of this composite system depend on the initial state of the measured system Q (which determines that possible values of A). One possible case is that the measured system Q is initially in an eigenstate $|k\rangle$ of observable A . In this case, acting the operator associated with observable A on our eigenstate will result in an eigenvalue a_k such that the evolution operator reduces to $e^{-\frac{i}{\hbar} \lambda a_k P}$. What this expression should indicate to us is that this operator acted on the initial pointer wave function $\phi(x = 0, t_i)$ will shift the pointer position by an amount λa_k . Then, immediately after the interaction between Q and M , the pointer wave function is $\phi(x = \lambda a_k, t_f)$. Thus the pointer wave function after measurement is still a narrow peak, but now it is centered at the position indicating the value of A . This is what is expected from an ideal measurement device.

However, this was in the case where the initial state of the measured system Q was an eigenstate of observable A . If we consider a different case, such as the initial state of Q being a superposition of two eigenstates

$$|\psi_o\rangle = c_0|0\rangle + c_1|1\rangle, \quad (6.3.3)$$

we can see that the initial state of the composite system $Q + M$ is the tensor product of the initial states of each sub system $|\psi_o\rangle \otimes |\phi\rangle$. Then, immediately after the interaction between Q and M , the state of the composite system becomes

$$|\psi\rangle = c_0|0\rangle \otimes |\phi_0\rangle + c_1|1\rangle \otimes |\phi_1\rangle. \quad (6.3.4)$$

Now, let us step back and make sense of this result. This wave function describing the composite system immediately after measurement is indicating that the final state of the pointer on the measurement apparatus does not go to definite position of either λa_0 or λa_1 as it would in any real life measurement. One way of attempting to make sense of this result is to say that the superposition quality the initial state of Q was transferred to the macroscopic apparatus itself. This is problematic in the sense that we have yet to obtain a definite result as we would expect

from any real life measurement. What von Neumann realized is that this issue cannot be put to rest by simply attaching a separate measurement device M' to the original as this would just result in the same situation of. One can attach as many new measurement devices as they choose, yet no amount of devices will resolve the issue of macroscopic interferences which have been transferred to the measurement device via the measured system Q . This result is called a *von Neumann chain*, and furthermore this model of measurement by von Neumann has greatly influenced the realm of quantum interpretation.⁴

6.3.1 Brief Discussion of Decoherence

One framework that can be applied to try and interpret this result of the von Neumann model is that of quantum decoherence. Although this will not be a rigorous presentation of decoherence, the following will still provide a conceptual picture of the theory, providing some kind of resolution to the issue of macroscopic interferences in the types of measurements considered in the previous section. For simplicity, let's assume that during the measurement process, the measured system Q is destroyed. Thus the final wave function for the apparatus as a function of the position x of the pointer is

$$\psi(x) = c_0\phi_0(x) + c_1\phi_1(x), \quad (6.3.5)$$

where $\phi_0(x)$ is a wave function for the pointer centered at position x_0 and similarly $\phi_1(x)$ is a wave function for the pointer centered at position x_1 macroscopically separate from x_0 . Something to consider here is that the coordinates assigned to the pointer positions are just one set of coordinates amongst many other possible coordinates that can describe the apparatus. Let's denote these other possible coordinates by variable y , and consider these coordinates as other possible mechanisms in our apparatus as well as any environmental factors that influence the device. Since we have said that the wave function of the pointer depends on these other coordinates describing the surrounding environment, we can more precisely write that the final

⁴The details of this section were greatly influenced by the work of Roland Omnès. See Omnès, *Understanding Quantum Mechanics* (Princeton University Press, 1999), 58-60.

wave function of the pointer is

$$\psi(x, y) = c_0\phi_0(x, y) + c_1\phi_1(x, y). \quad (6.3.6)$$

If one tries to imagine how a wave function like $\phi_0(x, y)$ or $\phi_1(x, y)$ may depend on environmental factors captured by y , it seems pretty clear that this function would be incredibly complicated for any realistic environmental setting. Additionally, one may expect that the phase of such a wave function is extremely sensitive to very slight changes in y . Thus due to the extreme sensitivity to the large array of y 's, one may also expect that the two final wave functions $\phi_0(x, y)$ and $\phi_1(x, y)$ could have very different and sensitive y dependencies. This claim would imply that for the same input value of y into each wave function, the two outputs could give drastically different results or phases, and furthermore these drastic phase differences would have no relation to each other. Due to the lack of relation between phases, we can imagine that the phase coherence between wave functions is effectively non-existent. Due to this complete lack of coherence in the phase of each wave function, it would seem legitimate to claim that over all possible y values, these two wave functions would average to zero. Another way to say this is that the two final wave functions for the pointer of the measurement apparatus are orthogonal in their y dependence such that

$$\langle \phi_0(x, y) | \phi_1(x', y) \rangle = \int \phi_0^*(x, y) \phi_1(x', y) dy = 0 \quad (6.3.7)$$

for any distinct pointer values x and x' . What this orthogonality of the y variable implies is that these macroscopic interferences transferred to the measurement device by system Q will destructively interfere due to the lack of phase coherence and thus be suppressed when making a measurement of the x variable. In principle, without rigorous presentation, this is the concept of Decoherence, or the suppression (and eventually absence) of macroscopic interferences. Now, the physical process in which interferences are destroyed is certainly a dynamical process, thus it must take some time to occur. The amount of time for decoherence to completely come into effect is the topic of lots of current research, but we know that it is an incredibly rapid and efficient process (perhaps even the most efficient and rapid in all of macroscopic physics). Given that it is such a fast process, one may wonder if an experimental device can be constructed to

observe decoherence in action, and the truth is yes it can, and has, been done, verifying the presence of the decoherence effect. Seeing that decoherence is a dynamical process that truly occurs in reality, this essentially provides closure to the von Neumann model of measurement, and thus we have a complete framework for how to understand quantum measurements even though our experimental results may still be quite curious and in need of deep analysis using quantum mechanics.⁵

⁵A more complete treatment of decoherence would provide a mathematical framework for explaining its dynamical nature. For a more complete discussion of the decoherence effect and measurements, see Omnès, *Understanding Quantum Mechanics* (Princeton University Press, 1999), 73-76 and 196-234.

7

Conclusion

Learning is not a completely linear process. This is true for many subjects, and is certainly true when it comes to studying quantum mechanics. Many introductory texts on the subject try and create linear pathways through the field in order to present a kind of story to the student in which each concept follows directly from the last. By doing so, an instructor hopes to create a web of ideas that the student can pull from in order to form their own understanding of the material. While there are many great resources and texts on the fundamentals of quantum mechanics, crafting these linear pathways is simply not reflective of the way people learn, and furthermore, not reflective of the way science is practiced. When doing experiments in a lab course, we often try to devise a step by step methodology that will take us from step 1 to the final step in a linear order. However, scientific experimentation outside of the classroom almost never occurs in this way. Rather, we look at a problem from various angles, we take some steps forward, we take some steps to the side, we reverse engineer, and we take breaks to solve other problems that will help with a particular aspect of an experiment. These kinds of human processes, which decentralize of our ideas in order to slowly narrow our focus onto one single question, are what make scientific experimentation and true creative innovation possible. The study of quantum mechanics, historically speaking, has functioned in this very same way. For instance, quantum theory was being put into practice in the lab well before the study of interpretation was regarded

as a promising and useful field. Thus scientists had to take some steps forward in the direction of experimentation before they realized that to better understand their results, they needed to go back and re-evaluate the philosophical foundations of quantum theory. In this way, trying to present quantum mechanics as a completely linear practice is doing a disservice to the future physicist who will quickly learn that engaging in a creative scientific practice is fundamentally non-linear.

With this in mind, the goal of this thesis was to present a couple of fundamental aspects of quantum mechanics in an explicit manner that strays away from the common formulations found in many introductory texts on quantum mechanics. Certainly the mathematical formalisms are the same, just presented in a manner that places the importance of conceptual and philosophical understanding ahead of mathematical rigor. Although this hierarchy of ideas may be present, one can see fairly easily that there is no lack of mathematical rigor in the presentation of this material, rather the mathematics functions as a bridge between physical phenomena observed in the lab and the philosophical foundations of quantum mechanics. Moreover, by presenting the subjects of entanglement and non-locality in the context of quantum optics experiments, the student will not only gain the mathematical tools needed to understand quantum mechanics, but will also gain the knowledge and experience needed to perform optics experiments in general. This is truly an example of how a non-linear learning trajectory can generate unique pathways towards understanding a variety of subjects which may or may not be interrelated. Furthermore, by studying quantum mechanics in this way, one realizes that the field of quantum optics can be utilized as a creative tool for revealing the subtle nature of quantum phenomena. When one utilizes this creative tool, they can discover for themselves the unity and totality of quantum mechanics as a theory that describes the physical universe. This kind of learning could be called “learning by self-discovery”, but certainly requires much more than just the self. It requires studying the ideas of those before us, the right, the wrong, the well accepted, the not so well accepted, and using the plasticity of our own minds to try to understand if things could be otherwise. This is, in principle, the motivating question behind the types of experiments

presented in this text, “Could physical reality possibly work in a different way than our theories tell us? Let’s find out.”

There are many more experiments of this nature that can be conducted to investigate these kinds of questions rooted in epistemology. For example, one experiment that we started but did not have time to finish was the Quantum Eraser test. In short, this is another experiment revealing the non-local nature of entangled systems, and can be performed by adding a Mach-Zehnder Interferometer to one arm of the SPDC apparatus described in chapter 4. As well, these single photon interferometers are essentially playgrounds in which one can study the non-local nature of correlated systems in a variety of ways. One such way is to use phase shifters on one particle to see how its correlation with another particle is effected. This would be another demonstration of non-local effects. In conclusion, I hope that this text has provided ample evidence that not only is quantum optics a wonderfully rich area in which to study the fundamentals of quantum mechanics, but that by studying concepts such as entanglement and Bell inequalities in this way, the student actually gains a wider and fuller perspective on the inner-workings of quantum theory.

8

Appendix

8.1 Appendix A. Digitizer Settings

To acquire data, a CAEN DT5725 Desktop Digitizer along with the CoMPASS software provided by CAEN was used to convert analog electronic signals from each Single Photon Counting Module (SPCM) to digital time-stamped data which was used to count the singles count rate per second for each detector as well as the coincidences counts per second between various detectors. Using the CoMPASS software, the digitizer settings could be manipulated for a variety of different parameters, all of which serve different and important purposes depending on the type of experiment being conducted. When the user opens the CoMPASS software, they should first fully connect the digitizer to the computer and power supply as laid out in the digitizer manual provided by CAEN. Once CoMPASS connects to the digitizer, the “Acquisition” tab will pop up and should look something like Fig. 8.1.1.

Notice that under “Acquisition settings” there is an option to have timed runs. This was very useful when we wanted to collect data for a specific amount of time. Under “List saving” we chose to save the raw and unfiltered data for each channel in separate CSV files for easy manipulation when it came time to do data analysis. According to the CAEN digitizer manual, **raw data** are classified as all events picked up by the digitizer including pile-up and saturation events. Additionally, **unfiltered data** are events acquired by the digitizer excluding the pile-up and

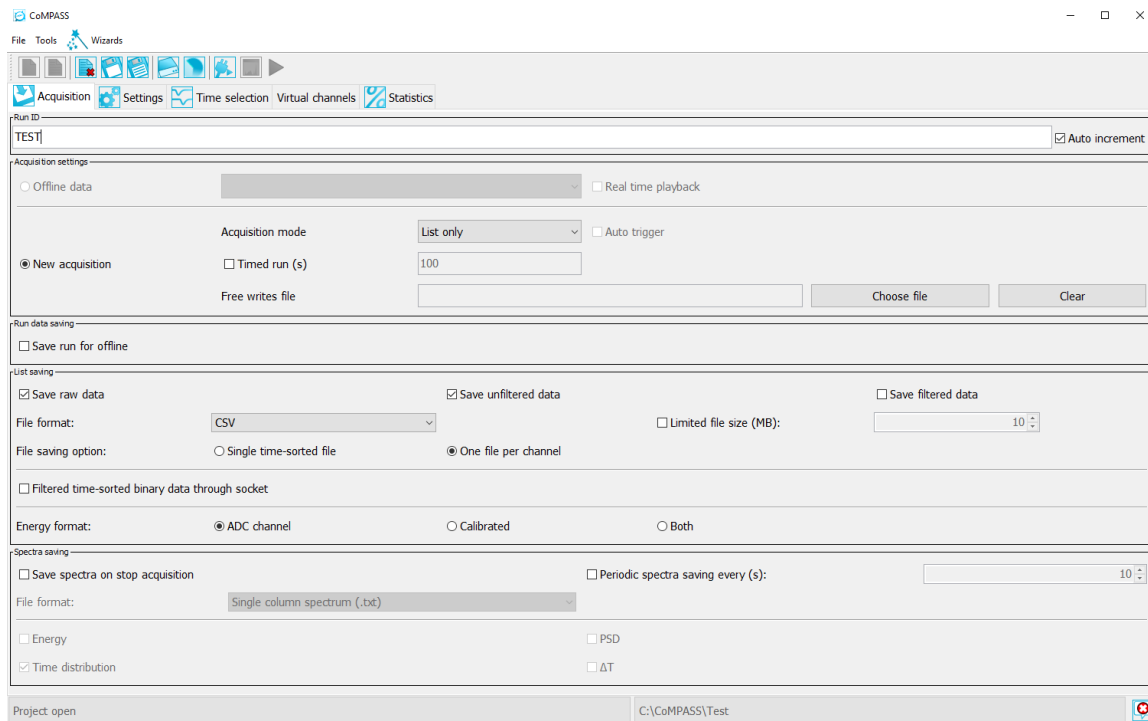


Figure 8.1.1. The Acquisition window is used to determine the time duration of the data collection as well as various options for saving data. For easier data analysis, we recommend saving at least the raw data from each channel into individual CSV files. These files will be saved in the appropriate DAQ folder on your computer in excel files (or other default spreadsheet software).

saturation events, and **filtered data** are all events that pass the set filters in the “Rejections” tab of the Settings window. We chose to save the raw and unfiltered data in order to determine the amount of saturation and pile-up events occurring, but once all saturation and pile-up events were eliminated, we used only raw data for analysis purposes. The rest of the settings under this tab are either pre-set by the program or are not of particular interest for our needs. Under the “Settings” tab, there will be ten sub tabs that allow the user to set specific digitizer parameters. Of these, there are three sub tabs of particular interest for these experiments. First, under the “Input” sub tab, make sure each channel being used is enabled. Then, we found that the detectors were not saturated by incoming analog signals when the Pre-trigger was set to 48ns. Saturation was also avoided by setting the Input dynamic to 2.0Vpp as opposed to 0.5Vpp. As well, by the recommendation of the digitizer user manual, make sure the Calibrate ADC box is checked to ensure accurate measurements. Under the “QDC” tab, there are a number of options

for the Gate, Short gate, and Pre-gate. The technicalities of these different gates should be well understood by looking at the user manual to learn more about their individual functions. For our purposes, we found the best results (no saturation or other error codes) for Gate = 88ns, Short gate = 68ns and Pre-gate = 48ns. These gate settings are essential to obtaining clean data, and so we stress that the user should refer to the digitizer manual to understand their respective functions. The next important sub tab is the Onboard Coincidence tab that allows the user to enable Coincidence mode and set the coincidence window.

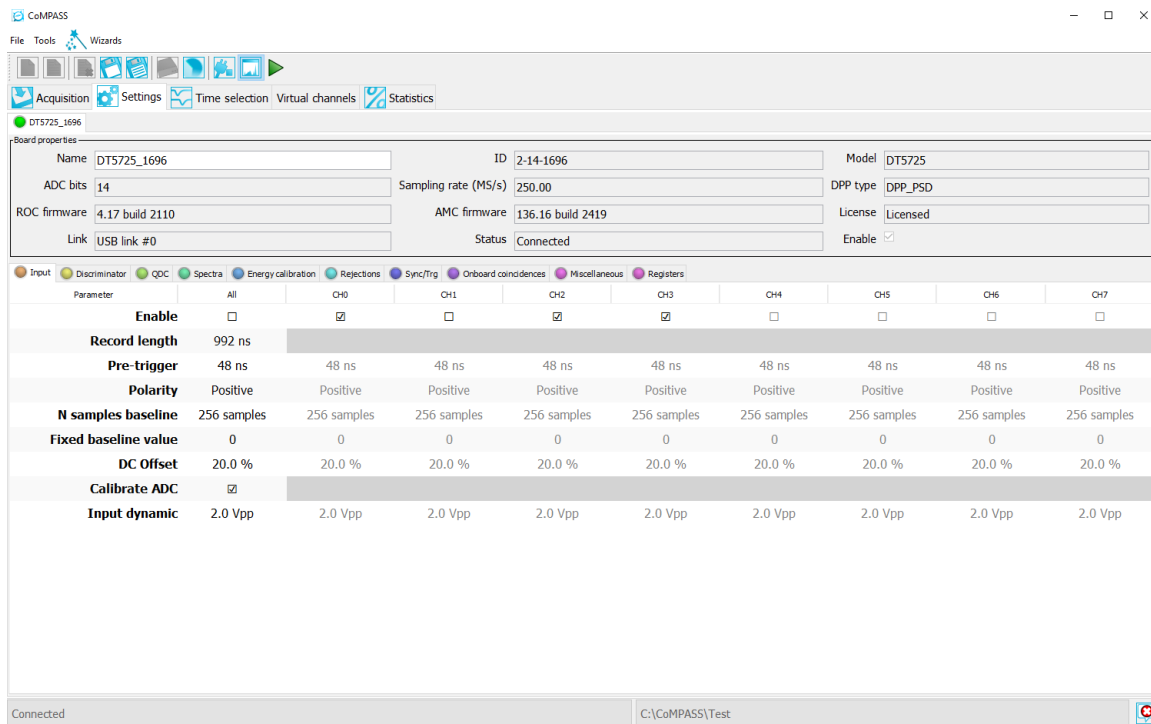


Figure 8.1.2. Input sub tab under the Settings tab. Make sure that the channels being used to collect data are enabled. Additionally, set the Pre-trigger and Input dynamic appropriately. By the user manual recommendation, enable Calibrate ADC so that the digitizer self calibrates each time it is turned on.

Although coincidence counting was more formally done using a MATLAB script, this function is useful when trying to quickly determine whether or not enough coincidences are being generated at detected. Given that the SPCM's send an analog pulse of approximately 10ns, the user can determine what size coincidence window suits their purposes. When taking data, the user can see a live plot of the singles (or coincidences) per second at each detector by opening an MCS graph for each channel of interest.

The screenshot shows the CoMPASS software interface. The 'Settings' tab is active, and the 'QDC' sub-tab is selected. The board properties section shows the following information:

Name	DT5725_1696	ID	2-14-1696	Model	DT5725
ADC bits	14	Sampling rate (MS/s)	250.00	DPP type	DPP_PSD
ROC firmware	4.17 build 2110	AMC firmware	136.16 build 2419	License	Licensed
Link	USB link #0	Status	Connected	Enable	<input checked="" type="checkbox"/>

Below the board properties, there is a table of gate settings for channels CH0 through CH7. The table has columns for 'Parameter' and 'All' channels, and rows for 'Energy coarse gain', 'Gate', 'Short gate', and 'Pre-gate'.

Parameter	All	CH0	CH1	CH2	CH3	CH4	CH5	CH6	CH7
Energy coarse gain	40 FC/(LSB x Vpp)	40 FC/(LSB x Vpp)	40 FC/(LSB x Vpp)	40 FC/(LSB x Vpp)	40 FC/(LSB x Vpp)	40 FC/(LSB x Vpp)	40 FC/(LSB x Vpp)	40 FC/(LSB x Vpp)	40 FC/(LSB x Vpp)
Gate	88 ns	88 ns	88 ns	88 ns	88 ns	88 ns	88 ns	88 ns	88 ns
Short gate	68 ns	68 ns	68 ns	68 ns	68 ns	68 ns	68 ns	68 ns	68 ns
Pre-gate	48 ns	48 ns	48 ns	48 ns	48 ns	48 ns	48 ns	48 ns	48 ns

The status bar at the bottom shows 'Connected' and the file path 'C:\CoMPASS\Test'.

Figure 8.1.3. The QDC sub tab under the Settings tab is used to set the gate, pre-gate and short gate. Refer to the digitizer user manual to learn more about the proper conditions placed upon the pre-gate and short-gate relative to the gate setting.

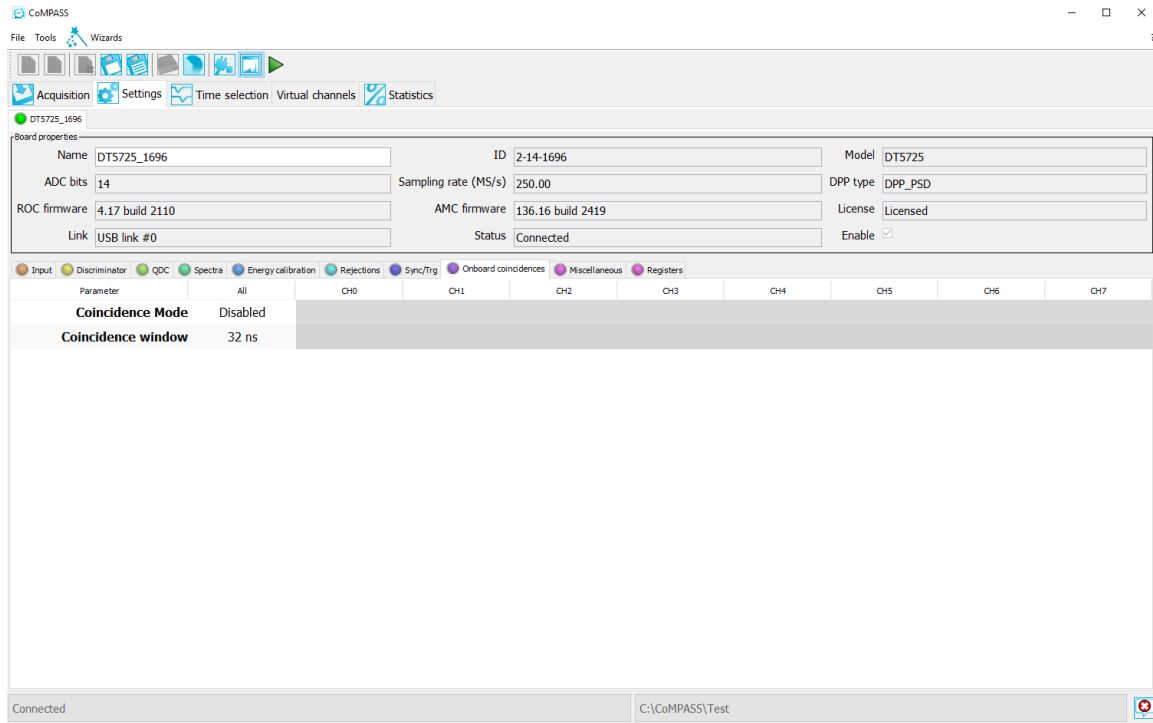


Figure 8.1.4. For data visualization purposes, and verifying the presence of down-converted pairs, use the Onboard Coincidence tab to enable Coincidence mode and set the coincidence window. Note that this window setting will determine the number of expected accidental coincidences.

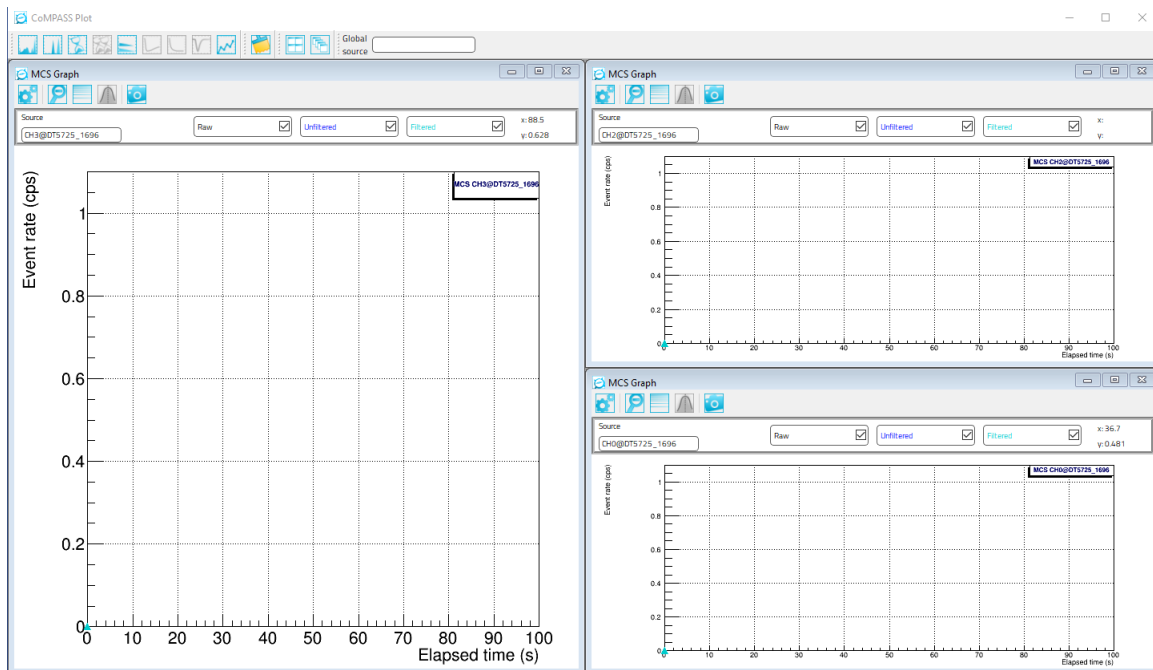


Figure 8.1.5. Displayed is an example of having three separate MCS graphs for each enabled channel. These are empty plots meaning no data is being taken. The axes displayed are counts per second (cps) as a function of time (in seconds).

This is useful when trying to maximize signals counts as well as to compare results from the coincidence counting script to the digitizer results. Using these settings, one should be able to collect clean and unsaturated singles counts and coincidence counts. In the end, collecting only the singles counts per second on each detector was needed as coincidence counts were calculated separately using MATLAB.

8.2 Appendix B. Quartz Crystal Thickness

With two thinly cut BBO crystals placed back to back, some of the pump photons will be down-converted in the first crystal and others in the second crystal. There is a time delay between the down-conversion that occurs in the first and second crystal. Because of this time delay, the paths of the photons are distinguishable ruining the purity of the entangled state that one hopes to generate using these two crystals. By delaying the component of the pump photon that generates down-converted photons in the second crystal by the proper amount to compensate for this time delay, the paths of the photons that generate the pairs will become indistinguishable thus ensuring the correlations between the photons. We calculate this time delay by considering the case where a photon is down-converted in the first crystal and then the other case where a pump photon goes through the first crystal and generates a down-converted pair in the second crystal.

1) Pump Photon Down-converted in Crystal 1

The velocity of the down-converted photon in the first crystal is

$$v_{dc} = \frac{c}{n_{dc}} \quad (8.2.1)$$

where c is the speed of light in vacuum and n_{dc} is the index of refraction of the BBO crystal for a down-converted photon of a particular wavelength.

Then, the time that the down-converted photon spends in the crystal is

$$t_{dc} = \frac{d}{v_{dc}} \quad (8.2.2)$$

where $d = 0.5mm$ is the crystal thickness.

2) Pump photon is not down-converted in Crystal 1

With a very similar treatment as the first case, the velocity of the pump photon in the first crystal is

$$v_p = \frac{c}{n_p} \quad (8.2.3)$$

where now n_p is the index of refraction of the BBO for a pump photon of a particular wavelength.

Then, the time that the pump photon spends in the crystal is

$$t_p = \frac{d}{v_p}. \quad (8.2.4)$$

Knowing the time that down-converted photon and pump photon spend in the crystal respectively, the difference in time spent in the first crystal (the time we need to compensate) is

$$\Delta t = t_p - t_{dc} = \frac{d}{c}n_p - \frac{d}{c}n_{dc}. \quad (8.2.5)$$

This is the time difference that will need to be compensated by using a quartz crystal. Consider a polarization state where the pump photons are subject to the ordinary index of refraction and the down-converted photons are subject to the extraordinary index. Then

$$n_p t = n_o(\lambda_p = 405\text{nm}) = 1.6919 \quad (8.2.6)$$

and

$$n_{dc} = n_e(\lambda_{dc} = 810\text{nm}) = 1.5442. \quad (8.2.7)$$

With values for the indices of refraction of the BBO, the time delay in this situation is

$$\Delta t = \frac{d}{c}n_p - \frac{d}{c}n_{dc} = 247\text{fs}. \quad (8.2.8)$$

Then, in order for proper compensation by the quartz crystal, we must shift one component of the pump photon by an amount so that the spatial difference between these two components is minus the difference in distance traveled by the pump and down-converted photon in the BBO. When proper compensation is achieved, it will be as if there is no time delay between the creation

of down-converted pairs in the first BBO and the second. From empirical data, we know that the indices of refraction of quartz at 405nm are $n_{\text{eq}}(405\text{nm}) = 1.5569$ and $n_{\text{oq}}(405\text{nm}) = 1.5477$. Thus, the condition for proper compensation is

$$dn_{\text{p}} - dn_{\text{dc}} = d_{\text{q}}n_{\text{eq}} - d_{\text{q}}n_{\text{oq}}. \quad (8.2.9)$$

And so, the thickness of quartz crystal needed for this compensation is

$$d_{\text{q}} = \frac{dn_{\text{p}} - dn_{\text{dc}}}{n_{\text{eq}} - n_{\text{oq}}} = \frac{\Delta tc}{n_{\text{eq}} - n_{\text{oq}}} = 8.0\text{mm}. \quad (8.2.10)$$

Note that although this derivation does not use group velocity indices of refraction, the end results for Δt and d_{q} are still reasonably consistent with those calculated by Galvez on his “Mathcad worksheet” found on his website cited in the bibliography.

8.3 Appendix C. Relevant Parts List

Part name	Manufacturer	Model name/number
BBO crystal	Newlight Photonics	NCBBO5050-405(I)-HA3
Paired BBO	Newlight Photonics	PABBO5050-405(I)-HA3
Quartz Crystal	Newlight Photonics	QAR25550-A-AR405/810
810nm filters	Thorlabs	FB810-10
Fiber Collimation Package	Thorlabs	F220FC-780
Fiber Optics Cables	Thorlabs	M31L01
Single Photon Counting Module	Excelitas Technologies	SPCM-EDU CD3375H
Desktop Digitizer	CAEN	DT5725
HeNe Laser (635nm)	Thorlabs	HNLS008L
GaN diode laser (405nm)	Unknown	Unknown

Table 8.3.1. These are all of the most relevant parts used in these experiments. Other less important parts such include polarizers, half-wave plates, mirrors, beamsplitters, and mounting hardware. The specific make and model of these less relevant parts is up to the user, but do make sure the optical elements are designed for proper the wavelength of light.

Bibliography

- [1] Benjamin Schumacher and Michael Westmoreland, *Quantum Processes, Systems, & Information*, Cambridge University Press, New York, 2010.
- [2] David Griffiths and Darrel Schroeter, *Introduction to Quantum Mechanics*, Cambridge University Press, New York, 2018.
- [3] Roland Omnès, *Understanding Quantum Mechanics*, Princeton University Press, Princeton, New Jersey, 1999.
- [4] Mark Fox, *Quantum Optics: An Introduction*, Oxford University Press, New York, 2006.
- [5] Max Jammer, *The Philosophy of Quantum Mechanics*, John Wiley & Sons, Inc., United States of America, 1974.
- [6] Olival Freire Junior, *The Quantum Dissidents: Rebuilding the Foundations of Quantum Mechanics (1950-1990)*, Springer, 2015.
- [7] David Bohm, *On Creativity*, Routledge, New York, 1998.
- [8] John S. Bell, *Speakable and unspeakable in quantum mechanics*, Cambridge University Press, New York, New York, 1987.
- [9] Enrique J. Galvez, C. H. Holbrow, M. J. Pysher, J. W. Martin, N. Courtemanche, L. Heilig, and J. Spencer, *Five quantum mechanics experiments for undergraduates*, American Journal of Physics **73** (2005), 127-140.
- [10] Guy Blaylock, *The EPR paradox, Bell's inequality, and the question of locality*, American Journal of Physics **78** (2010), 111.
- [11] John S. Bell, *On the Einstein Podolsky Rosen Paradox*, Physics **1** (1964), 195-200.
- [12] Enrique J. Galvez, *Quantum optics laboratories for teaching quantum physics*, Proceedings of SPIE **11143** (2019).
- [13] Daniel Schroeder, *Entanglement isn't just for spin*. arXiv:1703.10620v1 [physics.ed-ph].
- [14] Erwin Schroedinger, *Discussion of Probability Relations between Separated Systems*, Proceedings of the Cambridge Philosophical Society **31** (1935), 555.
- [15] Enrique J. Galvez, *2010, unpublished*. http://egalvez.colgate.domains/web/research/Photon/root/photon_quantum_mechanics.htm.

[16] Deady M., 2021. private communication.